Journal Pre-proof

Fecal microbiota transplantation for recurrent *Clostridioides difficile* infection associates with functional alterations in circulating microRNAs

Tanya M. Monaghan, Anna M. Seekatz, Nicholas O. Markham, Tung On Yau, Maria Hatziapostolou, Tahseen Jilani, Niki Christodoulou, Brandi Roach, Eleni Birli, Odette Pomenya, Thomas Louie, D. Borden Lacy, Peter Kim, Christine Lee, Dina Kao, Christos Polytarchou

PII: S0016-5085(21)00577-1
DOI: https://doi.org/10.1053/j.gastro.2021.03.050
Reference: YGAST 64242

To appear in: *Gastroenterology*
Accepted Date: 23 March 2021

Please cite this article as: Monaghan TM, Seekatz AM, Markham NO, Yau TO, Hatziapostolou M, Jilani T, Christodoulou N, Roach B, Birli E, Pomenya O, Louie T, Lacy DB, Kim P, Lee C, Kao D, Polytarchou C, Fecal microbiota transplantation for recurrent *Clostridioides difficile* infection associates with functional alterations in circulating microRNAs, *Gastroenterology* (2021), doi: https://doi.org/10.1053/j.gastro.2021.03.050.

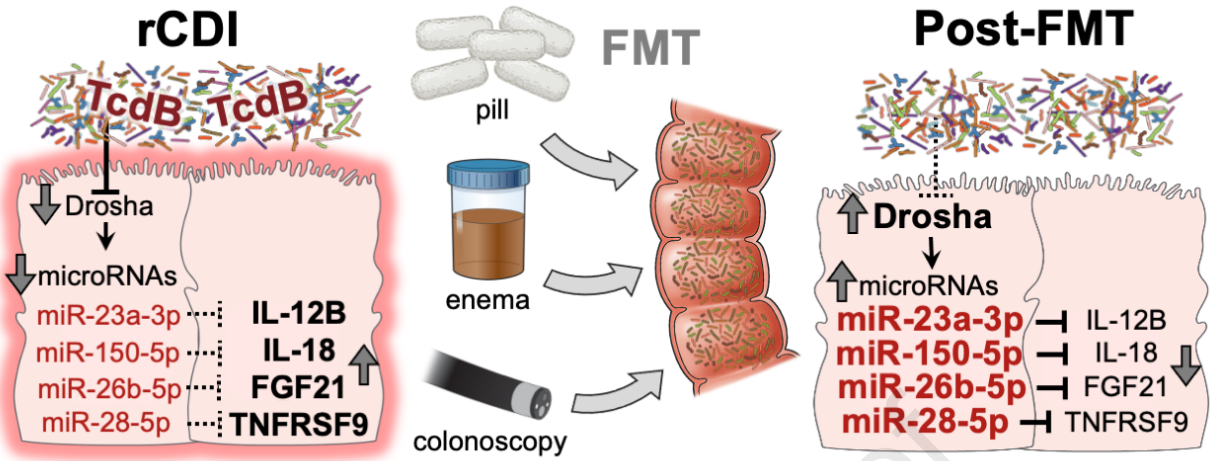

Fecal microbiota transplantation for recurrent *Clostridioides difficile* infection associates with functional alterations in circulating microRNAs

Tanya M. Monaghan[1,2*], Anna M. Seekatz[3#], Nicholas O. Markham[4,5#], Tung On Yau[6#], Maria Hatziapostolou[6#], Tahseen Jilani[7], Niki Christodoulou[6], Brandi Roach[8], Eleni Birli[6], Odette Pomenya[6], Thomas Louie[9], D. Borden Lacy[10], Peter Kim[11], Christine Lee[12,13], Dina Kao[8*], Christos Polytarchou[6*]

[*]Shared corresponding authorship

[#]Equal contribution

[1]NIHR Nottingham Biomedical Research Centre, University of Nottingham, Nottingham, UK

[2]Nottingham Digestive Diseases Centre, School of Medicine, University of Nottingham, Nottingham, UK

[3]Department of Biological Sciences, Clemson University, Clemson, South Carolina, USA

[4]Department of Medicine, Vanderbilt University Medical Center, Nashville, Tennessee, USA

[5]Epithelial Biology Center, Vanderbilt University School of Medicine, Nashville, Tennessee, USA

[6]Department of Biosciences, John van Geest Cancer Research Centre, Centre for Health Aging and Understanding Disease, School of Science and Technology, Nottingham Trent University, Nottingham, UK

[7]Advanced Data Analysis Centre, School of Computer Science, University of Nottingham, Nottingham, UK

[8]Department of Medicine, University of Alberta, Edmonton, Alberta, Canada

[9]Department of Microbiology and infectious Diseases, University of Calgary, Calgary, Alberta, Canada

[10]Department of Pathology, Microbiology, and Immunology, Vanderbilt University School of Medicine, Nashville, TN, USA; Veterans Affairs Tennessee Valley Healthcare System, Nashville, TN, USA

[11]Department of Mathematics and Statistics, University of Guelph, Ontario, Canada

[12]Vancouver Island Health Authority, Victoria, Canada

[13]Department of Pathology and Laboratory Medicine, University of British Columbia, Vancouver, BC, Canada

Contact information for corresponding authors

Dr Tanya M Monaghan

Clinical Associate Professor and Honorary Consultant Gastroenterologist

Anne McLaren Fellow

NIHR Nottingham Digestive Diseases Biomedical Research Centre

W/E 1381

E Floor, West Block

Queen's Medical Centre Campus

Derby Road

Nottingham, NG7 2UH

Tel: 0115 8231090

Fax: 01158231409

Tanya.Monaghan@nottingham.ac.uk

Dr Christos Polytarchou

Associate Professor

John van Geest Cancer Research Centre,

School of Science and Technology,

Nottingham Trent University,

Clifton Lane

Nottingham, NG11 8NS

Tel: 0115 8483215

Christos.Polytarchou@ntu.ac.uk

Dr Dina Kao

Associate Professor

Division of Gastroenterology, Department of Medicine

University of Alberta

8540-112 St

Edmonton, Alberta

T6G 2X8

780-492-8307

dkao@ualberta.ca

Acknowledgements

We are grateful to the participants that have made this research possible. We are grateful to Matt Emberg, Melanie Lingaya and Yirga Falcone for their technical assistance in sample preparation. This work was supported by a University of Nottingham Research Priority Area (RPA) grant to T.M.M. and supplemented by the National Institute for Health Research (NIHR) Nottingham Digestive Diseases Biomedical Research Centre based at Nottingham University Hospitals NHS Trust and University of Nottingham, Litwin Initiative at the Crohn's and Colitis Foundation to C.P, NTU Quality Research (QR) funds to C.P. and M.H., Micheal Smith Health Research Foundation to C. L., the National Institute for Diabetes and Digestive and Kidney Diseases (NIDDK) grant K01–DK111794 to A.M.S, as well as research funding provided by Alberta Health Services and University of Alberta Hospital Foundation to D.K.

The funders were not involved in study design, writing the report or decision for publication.

Author contributions

T.M.M., C.P. and D.K. designed the study, analyzed the data and wrote the paper. AM.S., N.O.M, TO.Y., M.H., N.C., E.B., O.P. and C.P. performed the experiments. T.J. and TO.Y. performed statistical analyses. D.K., T.L., B.R., CL., and P.K. developed the clinical sample cohorts. D.B.L. with N.O.M. provided access to human colonoids and purified whole C. difficile toxins. AM.S., N.O.M, M.H., D.B.L., CL. T.L., T.J., and P.K. provided intellectual input. All authors reviewed the manuscript and approved the manuscript in its final form.

Competing Interests statement

T.M.M. is a consultant advisor for Takeda. The remaining authors declare no competing interest.

Abstract

Background and aims

The molecular mechanisms underlying successful fecal microbiota transplantation (FMT) for recurrent *Clostridioides difficile* infection (rCDI) remain poorly understood. The primary objective of this study was to characterize alterations in microRNAs (miRs) following FMT for rCDI.

Methods

Sera from two prospective multicentre randomized controlled trials were analyzed for miRNA levels using the Nanostring nCounter platform and quantitative RT-PCR. Additionally, rCDI-FMT and toxin-treated animals and *ex vivo* human colonoids were employed to compare intestinal tissue and circulating miRNAs. miRNA inflammatory gene targets in colonic epithelial and peripheral blood mononuclear cells were evaluated by qPCR and 3'UTR reporter assays. Colonic epithelial cells were employed for mechanistic, cytoskeleton, cell growth and apoptosis studies.

Results

miRNA profiling revealed upregulation of 64 circulating miRNAs 4- and 12-weeks following FMT compared to screening, of which the top 6 were validated in the discovery cohort by RT-qPCR. In a murine model of relapsing-CDI, RT-qPCR analyses of sera and cecal RNA extracts demonstrated suppression of these miRNAs, an effect reversed by FMT. In mouse colon and human colonoids, TcdB mediated the suppressive effects of CDI on miRNAs. CDI dysregulated Drosha, an effect reversed by FMT. Correlation analyses, qPCR and 3'UTR reporter assays revealed that miR-23a, miR-150, miR-26b, miR-28 target directly the 3'UTR of IL12B, IL18, FGF21 and TNFRSF9, respectively. miR-23a and miR-150 demonstrated cytoprotective effects against TcdB.

Conclusion

These results provide novel and provocative evidence that modulation of the gut microbiome via FMT induces alterations in circulating and intestinal tissue miRNAs. These

findings contribute to a greater understanding of the molecular mechanisms underlying FMT and identify new potential targets for therapeutic intervention in rCDI.

Keywords

Fecal transplantation, *C. difficile*, microRNA, Drosha

Introduction

Fecal microbiota transplantation (FMT) is a well-established treatment for recurrent *Clostridioides difficile* infection (rCDI). Accumulating evidence also supports FMT as a potential treatment for other disorders associated with intestinal dysbiosis, including inflammatory bowel diseases, cancer, metabolic syndrome, and neuropsychiatric disorders.[1]

Despite the effectiveness of FMT in rCDI, its mechanisms of action remain poorly explored. Current evidence suggests the success of FMT may be attributed in part to the reconstitution of intestinal microbiota, restoration of secondary bile acid metabolism, and modulation of immune-mediated inflammatory responses.[2-3] We have previously reported effective FMT for rCDI is associated with activation of the bile acid-farnesoid X receptor (FXR)-fibroblast growth factor (FGF) pathway and decreased serum C-X-C motif chemokine 11 (CXCL11), interleukin-18 (IL-18), tumor necrosis factor-related activation-induced cytokine (TRANCE), IL-12B, CXCL6, and tumor necrosis factor receptor superfamily member 9 (TNFRSF9). [4] The gut microbiota can modify host cell responses to stimuli (e.g., metabolites) through alterations in the host epigenome and, ultimately, gene expression.[5] MicroRNAs (miRNA) are thought to be one way in which the gut microbiota communicates with the human host. These short non-coding RNA molecules (containing about 22 nucleotides) are expressed as individual genes or as parts of longer transcripts and are processed by machinery involving Drosha and Dicer nucleases, which generates the mature miRNAs. Mature miRNAs are loaded on argonaute (Ago)-containing complexes and bind to complementary sequences in the 3-untranslated region (3UTR) of messenger RNAs (mRNAs), resulting in transcript degradation and translational suppression of target genes. [6] Bacterial pathogens clearly alter host microRNA (miRNA) expression,[7] but less is known regarding the effect of commensal bacteria on the host microRNAome. A recent study has demonstrated how host fecal miRNAs, normal components of feces, can enter certain bacteria (e.g., *F. nucleatum* and *E. coli*) and regulate bacterial gene transcription and growth.[8] However, the alterations

in circulating miRNAs of rCDI patients undergoing FMT and the functional effects they may exert on downstream targets remain unknown.

Herein, we characterize the impact of FMT on circulating miRNA signatures to better understand immunological mechanisms relevant to FMT in the treatment of rCDI. Our findings suggest a conserved mechanism involved in regulating host miRNAs by *Clostridioides difficile* and identify new miRNA inflammatory targets in response to FMT.

Materials and Methods

Participants clinical data, sample collection and storage

Randomly selected rCDI subjects participating in 2 clinical trials (capsule vs colonoscopy delivered FMT [9] and fresh vs frozen enema-delivered FMT[10]) comprised the discovery and replication cohorts, respectively. Blood samples were collected between October 2014 and December 2016 (discovery cohort) and July 2012 and September 2014 (replication cohort) and stored at -80°C. Only sera with sufficient volume were selected for miRNA analysis. Healthy controls (n=42; mean [SD] age, 53.3 [20.7]; 30 women [71.4%] were defined as asymptomatic adults undergoing screening colonoscopy recruited from Edmonton, Canada. Clinical and demographic information were collected from medical records. Participant baseline characteristics are shown in Table 1. All participants provided written informed consent under the approvals granted by the research ethics boards of the University of Alberta (Pro 1994 and 49006), St. Joseph's Healthcare (#11-3622), and Hamilton Health Sciences (#12-505) in Canada.

Mouse model of rCDI

A mouse model of rCDI was used to assess miRNA, mRNA and protein levels following infection and treatment with FMT, as described previously.[11] Animal work was approved by the Clemson University Institutional Animal Care and Use Committee (IACUC). Additional details are available in the Supplementary methods. Briefly, 6-8 week old

C57BL/6 mice were given 0.5 mg/mL cefoperazone (MP Biochemicals, cat# 199695) in sterile drinking water (Gibco Laboratories, cat# 15230) ad libitum for five days (-7 days prior infection, n = 42). Two days after cessation of antibiotics, mice received 10^3 *C. difficile* strain 630 spores resuspended in 1mL sterile water, prepped as described previously (day 0, n = 36).[12] A subset of mice was euthanized 4 days post infection (dpi) to assess miRNA during acute infection (n = 9). The remainder of the mice received 0.4 mg/mL vancomycin (Sigma, cat# V2002) on 4 dpi for 5 days (4-9 dpi) ad libitum in sterile drinking water (n = 27). On 11 dpi, FMT prepped from untreated (n = 8), healthy age-matched mice (mFMT) was administered via oral gavage to a group of mice. Each mouse received 100 µL of FMT material diluted in phosphate-buffered saline (PBS); (~0.2 grams fresh fecal material in 1.5 mL pre-reduced PBS, homogenized via mixing and gravity filtering). One group of mice received all antibiotics and mFMT but no *C. difficile* inoculum (handling and experimental control, n = 6). The remainder of infected mice (n = 12) did not receive FMT (noFMT). Fecal sampling was conducted throughout the experiment, and endpoint cecal sampling, to assess *C. difficile* load, was determined by plating 20µL of content from individual samples in 1:10 PBS solution and serially diluted on taurocholate cycloserine cefoxitin fructose agar (TCCFA) under anaerobic conditions (Coy Laboratory Products, Grass Lake, MI, USA). The CFU/mL content was determined after overnight incubation at 37 °C. Mice were euthanized on 21 dpi and cecal contents, tissue and serum were flash frozen in liquid nitrogen and kept at -80°C for downstream analyses.

Mouse toxin challenge model

The animal protocol was approved by the Vanderbilt University Medical Center IACUC. 6-8 week old C57BL/6 mice (Jackson Labs) were observed upon arrival to ensure normal health. Mice were separated into three groups (n = 6 per group) to receive intrarectal instillations of either purified recombinant whole TcdB, TcdA and TcdB, or Hank's Balanced Salt Solution (HBSS) vehicle control, as described elsewhere.[13] Further details on the purification of the toxins are described in the Supplementary methods. Toxins

were derived from the VPI 10463 *C. difficile* reference strain and prepared as 15 µg in a total volume of 100 µL per instillation. Mice were anesthetized with isofluorane and confirmed to be sedated by toe pinch. One mL of HBSS was instilled intrarectally to evacuate stools with a flexible plastic gavage applicator (20G x 30MM, gavageneedle.com). Instillation was performed over 30 sec while lightly pinching closed the anus, which was held for an additional 30 sec as previously described.[13] Mice were returned to cages to recover. After two-to-five hours, mice were humanely euthanized by CO_2 inhalation and cervical dislocation. Whole blood was extracted via cardiac puncture and allowed to clot in an RNAse-free microcentrifuge tubes for 15 min at room temperature prior to centrifugation for 15 min at 1500 × g at 4°C. Serum was transferred to a fresh tube and flash frozen in liquid nitrogen. The colon was isolated and dissected from surrounding visceral tissue. The whole colon was washed in chilled, sterile 1x PBS before portions of the middle and distal colon were combined and flash frozen for protein and miRNA analysis.

Treatment of human colonoids with *C. difficile* toxins

Deidentified human colon tissue was obtained through the Cooperative Human Tissue Network. On the day of colon resection surgery, normal marginal colon mucosa was resected and placed into Dulbecco's Modified Eagle Medium (DMEM) at 4°C. Within hours, the tissue was prepared into normal human colonoids with Intesticult Organoid Growth Medium (Stem Cell Technologies) using the manufacturer's protocol (https://cdn.stemcell.com/media/files/pis/DX21423-PIS_1_0_0.pdf). Colonoids were suspended in Matrigel matrix (Corning) with standard growth factor concentration for maintenance and passage. Matrigel with reduced growth factors was used for suspending colonoids in the final passage for the experiment. Eight hours prior to toxin exposure, organoids were serum-starved with DMEM and no growth serum. Colonoids were exposed to TcdA (10 pM), TcdB (10 pM), or DMEM vehicle negative control for either 30 min or 6 hours. Colonoid-containing Matrigel was washed once with 1x PBS and flash frozen in liquid nitrogen for protein analysis. For miRNA analysis, colonoids were

removed from Matrigel using Gentle Cell Dissociation Reagent (Stem Cell Technologies) and resuspended in RNAlater (Invitrogen). Colonoids in RNAlater were stored at 4°C overnight before freezing at -80°C.

Serum miRNA isolation and high-content analysis

Human serum was isolated by centrifugation (2200 g for 10 minutes at room temperature) from whole blood and snap-frozen. RNA was isolated from human and animal serum samples (200 µL) using the miRNeasy Serum/Plasma Kit (Qiagen) according to the manufacturer's instructions. Eluted RNA from serum samples was further purified and concentrated by using Amicon Ultra YM-3 columns (3000 kDa MWCO; Millipore).

For high-content miRNA analysis, RNAs following hybridization reactions were processed using the nCounter Prep Station and nCounter Digital Analyser. miRNA levels (n = 800) were analysed using the nSolver software, v3.0 (Nanostring Technologies Inc, Seattle, WA, USA). Normalisation was performed using all miRNAs (n = 110) with coefficient of variation less than 70%.[14]

Additional information is available in the Supplementary Materials and Methods section.

Statistical analysis

All statistical analyses were performed in SPSS v.24 and R 3.5.1. Descriptive statistics for participant characteristics at baseline were reported using mean and standard deviation and percentages. All data are expressed as mean and s.e.m. Systematic within-week changes for each miRNA were examined using a non-parametric longitudinal method (nparLD in R package) followed by Wilcoxon signed-rank test for pairwise comparisons. The association between the metavariables and miRNAs was assessed using Spearman correlation. Heatmaps for capsule and colonoscopy combined and separately for capsule and colonoscopy delivered FMT were generated in R package ComplexHeatmap2.[15] Normality was checked using the Kolmogorov-Smirnov test. Graph generation, fold changes and statistical significance in levels of circulating miRNAs were

assessed by qPCR using OriginPro and Wilcoxon matched-pairs signed rank test. Significance differences were considered when *P< 0.05. ** P < 0.01, *** P < 0.001.

Results

FMT modifies circulating miRNAs in rCDI patients

For miRNA profiling, we first analysed serum samples derived from the discovery cohort.[9] Table 1 describes patient baseline characteristics. Sera obtained at screening, 4- and 12-weeks post-FMT from 42 participants who achieved a clinical cure following FMT, were subjected to miRNA analysis using the Nanostring nCounter platform. miRNA profiling of 126 samples revealed the significant upregulation of 64 circulating miRNAs 4- and 12-weeks following FMT, compared to screening (Fig. 1A). The miRNAs with the highest levels detected are depicted in Fig. 1B. Comparable changes in miRNA levels were detected in recipients of either by capsule or colonoscopic FMT (Supplementary Fig. 1). Pathway enrichment analysis identified overlaps between the top three miRNA-regulated pathways, B-cell lymphoma 2 (Bcl-2), Runt-related transcription factor 2 [(RUNX2; linked to NF-kappa-B inhibitor beta (NFKBIB)] and phosphoinositide 3-kinase (PI3K reg class 1A p55-gamma), linking inflammatory signalling to immune cell survival and differentiation (Fig. 1C). Pathway analysis also uncovered commonalities with other diseases (e.g., inflammatory bowel disease and multiple sclerosis) and cell functions such as apoptosis (Supplementary Figures 2 and 3).

We next sought to validate our discovery cohort results. For the replication cohort, we assessed 24 patients at 3 time points: screening, at two and four weeks following FMT.[10] Table 1 describes patient baseline characteristics. The top 6 upregulated miRNAs from the discovery cohort analysis (Fig. 1B) were selected for RT-qPCR validation in our replication cohort. Individual miRNAs were found to be upregulated in 78-94% of samples analysed, with the average changes ranging between 3-and-12 fold (Fig. 1D).

FMT modifies intestinal tissue miRNAs in a mouse model of rCDI

The concerted increase of circulating miRNAs by FMT suggests that *C. difficile*-associated dysbiosis may regulate miRNAs through a conserved mechanism. We tested this hypothesis by employing a mouse model of rCDI.[8] Animals pre-treated with cefoperazone received 10^3 *C. difficile* spores, and 4 days post-infection (dpi) were exposed to vancomycin. At 11 dpi, a group of mice received fresh FMT derived from healthy mice. Sera collected 21 dpi were subjected to RT-qPCR. Parallel to what we found in rCDI patients, the same top 5 miRNAs (miR-4454 has not been characterised in mice) and in addition two potentially functional miRNAs were also upregulated after FMT. *C. difficile* recurrence (Supplementary Figure 4) resulted in downregulation of the tested circulating miRNAs in mice (Fig. 2A) concomitant with a decrease in animal body weight (Supplementary Figure 5). To examine the time-dependence of miRNA regulation by CDI, we assessed miRNA levels during the acute phase of infection (4 dpi). RT-qPCR analysis revealed that the suppression of circulating host miRNAs may be an early sign of CDI (Supplementary Figure 6). Importantly, the inhibitory effects of rCDI on miRNA levels was reversed 10 days post-FMT (Fig. 2A).

We next tested whether the circulating miRNA changes reflect the effects of rCDI on colonic tissue. RNA extracts from the ceca were analysed by RT-qPCR. Our results showed that tissue miRNA levels altered similarly to circulating miRNAs (Fig. 2B). Comparisons of the changes of individual microRNA levels in matched tissue and serum samples, from all animals, showed significant and positive correlation between circulating and ceca-expressed miRNAs (Supplementary Figure 7). This supports the notion that alterations in circulating miRNAs may be originating from colonic tissues. Furthermore, we found even stronger positive correlation between matched colonic and circulating miRNAs derived from an 84-year-old male patient with fulminant CDI treated with FMT by colonoscopy (Supplementary Figure 8). In mice, tissue miRNA levels downregulated by rCDI reached statistical significance in the early phase of infection (Supplementary Figure 9), while FMT upregulated the tissue miRNAs, coinciding with the

reduction of *C. difficile* load (Supplementary Figure 4) and the recovery of animal body weight (Supplementary Figure 5).

Toxin B suppresses miRNAs in the intestinal mucosa

C. difficile pathogenicity is primarily mediated by exotoxins that induce cell death. We investigated the effects of purified toxin A (TcdA) and toxin B (TcdB) on host miRNA regulation. Mice were treated by intrarectal instillation with a combination of TcdB and TcdA, TcdB alone (15µg), or vehicle (HBSS), and colonic tissues and sera were collected 2-5 hours post instillation. RT-qPCR analysis of serum RNA extracts showed the toxins had no effect on circulating miRNAs (Supplementary Figure 10). However, the expression of the same miRNAs was suppressed in colonic tissues of *C. difficile* infected mice. Notably, TcdB suppressed miRNA levels, an effect enhanced by its combination with TcdA (Fig. 3A). The discrepancy between circulating and tissue miRNAs in this model suggests the impact of the toxins is luminally confined and may not lead to changes in circulating miRNA levels due to local and time-restricted exposure of animals to toxins in early time points (2-5 hours).

The above findings suggest the effect of CDI on miRNA regulation is mediated by the direct effect of TcdA and/or TcdB on colonic epithelial cells and the observed alterations in circulating miRNAs in FMT-treated patients may result from changes at the tissue level. To test this hypothesis, we exposed normal human colon organoids (colonoids) to TcdA or TcdB and analysed miRNA expression. Colonoids from freshly isolated human colon mucosa were treated with TcdA (10 pM), TcdB (10 pM) or vehicle (DMEM), and cell extracts were obtained 30 min and 6 hours later. RT-qPCR analysis showed that 30 min after exposure to TcdB, all miRNAs studied were reduced (Fig. 3B), an effect sustained for 6 hours (Fig. 3C). These results show that miRNA suppression in CDI is attributed to

the activity of TcdB and further support the hypothesis that FMT-mediated upregulation of circulating miRNAs is driven, at least partly, at the epithelial level.

FMT counteracts *C. difficile* effects on miRNA biogenesis

The evidence collectively show that the miRNAs studied adhere to a common mode of regulation, albeit they are encoded by different genes and controlled by different mechanisms at the level of transcription. In fact, the miRNAs studied are located in different chromosomes, are intragenic (exonic or intronic) or intergenic, and their expression is under the control of distinct regulatory elements. Hence, their regulation may be a result of a universal mechanism. Following transcription, miRNA maturation is a process shared by most miRNAs, and their concerted upregulation by FMT suggests that miRNA processing may be affected by *C. difficile*-associated dysbiosis. Therefore, we analysed the effects of *C. difficile* and FMT on the expression of enzymes playing a central role in miRNA biogenesis (Drosha, Dicer1, Ago2). RT-qPCR analysis of cecal RNA extracts from rCDI mice suggested that CDI suppresses Drosha expression by 50% (Fig. 4A, left panel), with minor changes on Dicer1 and Ago2 mRNA levels (Supplementary Figure 11). A more pronounced effect (> 80% decrease) on Drosha expression was evidenced at the protein level (Fig. 4A, right panel). Importantly, the effects on both Drosha mRNA and protein were reversed by FMT (Fig. 4A). Similarly, in colonic tissues of mice treated with exotoxins, Drosha mRNA levels dropped by 40% (Fig. 4B). In human colonoids, TcdB showed small but significant effects on Drosha mRNA (Fig. 4C, left panel), while western blot analysis revealed a robust decrease (>60%) in protein levels (Fig. 4C, right panel).

To investigate the role of Drosha suppression in mediating the CDI effects on the regulation of miRNA levels we knocked down Drosha in colonic epithelial cells (NCM356) by means of siRNA. We verified that the knockdown of Drosha mimics the effects of TcdB on Drosha protein levels in these cells (Fig. 4D). RNA extracts from these cells were subjected to RT-qPCR for the levels of the primary transcripts (pri-miRNAs) and the mature forms of three different miRNAs, known to be transcriptionally regulated by

distinct mechanisms.[16-18] The results showed that upon Drosha inhibition the levels of the pri-miRNAs (Fig. 4E, upper panel) are increased with the concurrent and significant decrease in mature miRNA levels (Supplementary Figure 12). We then measured the levels of these primary transcripts in colonoids treated with TcdB. In the same line, we found that though the mature miRNAs are suppressed by TcdB (Fig. 3), the levels of the respective pri-miRNAs are increased (Fig. 4E, lower panel).

Combined, these data suggest that Drosha expression is decreased in response to CDI, a phenomenon regulated at both the transcriptional and post-transcriptional level. Furthermore, they attribute the concerted changes in miRNA levels to the dysregulation of miRNA biogenesis machinery (proposed model, Fig. 4E) by rCDI and its recovery by FMT treatment.

FMT-regulated miRNAs possess functional properties

We next investigated the downstream effects of FMT-regulated circulating miRNAs in our rCDI patient cohorts compared to healthy controls. We assessed miRNAs predicted to target specific chemokines and cytokines, which we previously found to be downregulated by FMT.[4] Based on TargetScan prediction analyses we found that the levels of 6 miRNAs in FMT-treated rCDI patients inversely correlate with the serum levels of FGF21, IL-12B, IL-18 and TNFRSF9 proteins (Supplementary Figure 13). miR-23a, miR-26b and miR-130a are predicted to target the 3'UTR of FGF21 mRNA, miR-23a is predicted to target the 3'UTR of IL-12B, miR-150 the 3'UTR of IL-18, while miR-20a and miR-28 are the 3'UTR of TNFRSF9. Overexpression of these miRNAs in colonic epithelial cells showed that miR-26b, miR-23a, miR-150 and miR-130a suppresses the mRNA levels of FGF21, IL-12B, IL-18 and TNFRSF9 respectively (Fig. 5A). These findings were further validated by 3'UTR reporter assays, where mutations in their target sequences within the 3'UTRs reversed their suppressive effects (Fig. 5B), suggesting that the four miRNAs directly target these mRNAs.

In addition to the changes observed for these miRNAs in the mouse model of rCDI (Fig. 2) human colonoids and mouse colonic tissues treated with TcdB (Fig. 3) and FMT-treated rCDI patients (Fig. 1A), we found rCDI decreases the levels of these four miRNAs in sera when compared to healthy controls (Fig. 5C). The use of miRNA inhibitors against miR-26b and miR-150, in PBMCs derived 4 weeks after FMT treatment, partly (FGF21) or completely (IL-18) reversed the effect of FMT on their expression, suggesting a functional role for these two miRNAs in FMT therapy (Supplementary Figure 14). Pre-treatment of colonic epithelial cells with these cytokines revealed that though FGF21, IL-12B and TNFRSF9 had no effects (Supplementary Figure 15), IL-18 sensitises cells to TcdB but not TcdA (Fig. 5D), an effect validated in a second mucosal cell line (Fig. 5E). The identified miRNA-target interactions provide novel links between inflammation and metabolism (Supplementary Figure 16).

FMT-regulated miRNAs modulate susceptibility to *C.difficile* toxin effects

We next examined whether miRNAs upregulated by FMT can affect the colonic epithelial response to *C.difficile* toxins. Firstly, we tested the effect of miRNAs up-regulation, alone or in combination with TcdB, on cell survival. The results showed that individual miRNAs had minor effects on TcdB cytotoxicity. However, combination of miR-23a-3p and miR-150-5p significantly increased cell survival (Fig. 6A). A live-cell analysis assay verified the above findings (Supplementary Figure 17) and suggested that miR-23a-3p and miR-150-5p alone (Supplementary Figure 18) or in combination confer a growth advantage to cells treated with TcdB (Fig. 6B). In accordance, the viability of a second mucosal cell line exposed to TcdB was significantly increased by the combined overexpression of miR-23a-3p and miR-150-5p (Fig.6C).

Although miR-23a-3p and miR-150-5p had minor effect on the early TcdB-mediated cytotoxicity they promoted cell survival (Supplementary Figure 19). Using a real-time Caspase3/7 detection assay, we found that TcdB induces cell apoptosis in a dose-dependent manner (Supplementary Figure 20). miR-23a-3p and miR-150-5p had additive effects in reducing susceptibility to TcdB-induced apoptosis over time (Fig. 6D).

A major cytopathic effect attributed to TcdB is the induction of cell morphological and cytoskeleton changes, which can be visualized by staining colonic epithelial cells with fluorescence conjugated phalloidin. Using this method, we observed major morphological changes to epithelial cells such as loss of actin stress fibres, spindle-like formation and cell rounding when exposed to both TcdA and TcdB. Quantification of the ratio of rounded and spindle-like cells, revealed that TcdB-induced cytopathic effects were significantly counteracted by the overexpression of miR-23a-3p and miR-150-5p (Fig. 6E, Supplementary Figure 21).

Discussion

We report the first study to examine the effects of FMT for rCDI on miRNA signatures. Our findings in a clinical rCDI cohort demonstrated the concerted regulation of miRNA expression by FMT. Validating these observations in a mouse model of rCDI and organoids, we provide evidence that miRNA processing in colonic epithelial cells is directly altered by *C. difficile* toxins and may be affected by *C. difficile*-associated dysbiosis. Conditional knockout of the miRNA-processing enzyme *Dicer* in murine intestinal epithelial cells, which secrete fecal miRNAs, has been shown to modulate the gut microbiota and exacerbate colitis. This phenotype can be rescued via wild-type fecal transplantation.[8] From this observation, we hypothesized that colitis due to CDI can suppress circulating miRNAs, which can be restored by FMT. In support of our hypothesis, predominant suppression of miRNAs was observed in two independent cohorts of rCDI patients but was differentiated from observed miRNA suppression in other colitis patient cohorts, such as in patients with chronic inflammatory bowel diseases (IBD; ulcerative colitis[14] and Crohn's disease[19]) and associated colorectal cancer.[20] For example, miR-30 family members are upregulated in both ulcerative colitis and Crohn's disease, but suppressed in rCDI, while miR-23a-3p is upregulated only in ulcerative colitis and downregulated in rCDI. These differences may be leveraged for future diagnostic purposes and could help identify IBD patients who can benefit from

biotherapeutic products such as FMT, which currently demonstrate variable efficacy compared to CDI patients.

The miRNA signature in the mouse models suggest that changes in circulating miRNAs reflect alterations in the intestinal epithelial cells. Importantly, the effects of *C. difficile* infection on miRNA levels are reversed in both sera and tissues after FMT, parallelling the post-FMT serum miRNA changes observed in patients with CDI following FMT. TcdA and TcdB have been causally linked to the pathogenetic mechanisms of CDI.[21] At the cellular level, toxins induce cytoskeleton reorganisation and tight junction disruption resulting in cell rounding and cell death.[22] Here, we show that TcdB suppresses key inflammation-related miRNAs in murine intestinal tissues and human colonoids. Moreover, we identify two miRNAs upregulated by FMT, miR-23a and miR-150, which exert cytoprotective effects against TcdB. Interestingly, we found that IL18, previously shown to contribute to mucosal damage[23], sensitizes colonic epithelial cells to TcdB. In addition, we show that IL18 is a direct target of miR-150, suggesting a new mechanism by which FMT may counteract *C. difficile*-induced epithelial disruption. Additional miRNA-regulated cytokines may be involved in the regulation of anti-inflammatory effects of FMT. We found that miR-23a targets IL12B, an essential activator of Th1 cell development, associated with CDI recurrence.[24] Collectively, these data support a role for miRNAs suppressed by toxins as a new pathogenic mechanism for CDI. We propose that the restoration of these miRNAs by FMT contributes to the protection of epithelial barrier integrity. Changes in circulating miRNAs may also contribute to extra-colonic manifestations of CDI including cardiac, renal, and neurologic impairment.[22]

Our analyses of the miRNA biogenesis machinery illustrate that downregulation of miRNAs is likely through the suppression of Drosha by CDI/TcdB and is restored following FMT. Inhibition of Drosha results in defective microRNA processing with accumulation of primary (unprocessed) miRNA transcripts. Our findings suggest the biphasic regulation of the microprocessor by CDI. The temporal effect of TcdB suggests that early miRNA regulation is attributed to a non-transcriptional mechanism. In fact,

Drosha protein is reduced in response to TcdB before its mRNA levels are suppressed. Different types of stress have been associated with the stability of Drosha protein. Under oxidative stress, Drosha is phosphorylated by p38 MAPK at the N-terminus. This results in disruption of its interaction with DGSCR8, relocation to the cytoplasm and protein degradation.[25] Indeed, the cytotoxic effect of TcdB has been shown to depend on assembly of the host epithelial cell NADPH oxidase (NOX) complex and the production of reactive oxygen species.[26] Other metabolic inputs may be involved. The mTOR nutrient/amino acid sensor activates MDM2 which catalyses Drosha ubiquitination marking it for degradation.[27] The long-term suppression of both Drosha mRNA and protein may involve a gene transcription regulatory mechanism. The transcription factor c-Myc activates *Drosha* gene and upregulates Drosha protein,[28] and is under the control of the Wnt/beta catenin pathway, which is suppressed by both toxins.[29-30]

The regulation of miRNA levels by *C. difficile* may not rely solely on the effects of toxins on mucosal cells. miRNA suppression, mediated by surface layer proteins of specific *C. difficile* ribotypes, has been proposed to attenuate the host's immune response resulting in a more persistent infection in mice.[31] Interestingly, the suppression of circulating miRNAs upon depletion of regulatory T cells (Tregs), reported in mouse models of autoimmune diseases,[32] suggest potential links between Treg function, CDI, miRNAs and FMT. Recent experimental evidence has linked the effectiveness of FMT for colitis with the induction of IL-10 and TGB-β, cytokines critical for Treg accumulation in the intestine.[33] Whether FMT-directed immunosuppression aids in the recovery from *C. difficile* requires further investigation.[3]

Intriguingly, in *C. difficile* naïve animals treated with FMT we observed a trend towards higher Drosha and Dicer mRNA levels and alterations in the miRNA profiles. These control animals were conditioned with cefoperazone (an antibiotic against both Gram-positive cocci and Gram-negative bacteria) to facilitate *C. difficile* colonization. This observation proposes that host-microbe interactions regulate the host miRNA biogenesis

machinery, which in turn may affect directly or indirectly, through the immune response, gut microbiota composition.

Here, we reported changes in circulating and colonic miRNAs in the context of FMT for rCDI, validating our observations across two independent randomized trials. Using two different animal models, human colonoids and colonic epithelial cells, we substantiated that *C. difficile* highjacks miRNA biogenesis and show how miRNA restoration contributes to the therapeutic effects of FMT. Our findings strongly support the need for further mapping of the epitranscriptomic changes associated with FMT. While our data in rCDI mice suggests that TcdB impacts Drosha rather than Dicer1 or Ago2 expression, studies with conditional knockout mice of the miRNA-processing machinery, such as *Dicer* or *Drosha*, may reveal additional molecular mechanisms or metabolic pathways affected by CDI-induced colitis.

Together, these results provide novel and provocative evidence that modulation of the gut microbiome via FMT induces changes in circulating miRNAs, and a subset of these miRNAs downregulates inflammatory protein expression and protects epithelial cells. These findings add new insight into the molecular mechanisms underlying *C. difficile* pathogenesis and FMT and identify new potential targets for therapeutic intervention.

References

1. D'Haens GR, Jobin C. Fecal Microbial Transplantation for Diseases Beyond Recurrent *Clostridium Difficile* Infection. *Gastroenterology* 2019; 157 (3): 624-636.
2. Khoruts A, Sadowsky MJ. Understanding the mechanisms of action of faecal microbiota transplantation. *Nat Rev Gastroenterol Hepatol* 2016; 13 (9): 508-16
3. Petri Jr, WA and Frisbee, AL. Considering the immune System during Fecal Microbiota Transplantation for *Clostridioides difficile* infection. Gastroenterology 2020; 26 (5): 496-506.

4. Monaghan T, Mullish BH, Patterson J, et al. Effective fecal microbiota transplantation for recurrent *Clostridioides difficile* infection in humans is associated with increased signalling in the bile acid-farnesoid X receptor-fibroblast growth factor pathway. *Gut Microbes.* 2019; 10 (2): 142-148.
5. Qin Y, Wade PA. Crosstalk between the microbiome and epigenome: messages from bugs. *J Biochem* 2018; 163 (2): 105-112.
6. Gebert LFR, MacRae IJ. Regulation of microRNA function in animals. Nat Rev Mol Cell Biol 2019; 20: 21-37
7. Aguilar C, Mano M, Eulalio A. MicroRNAs at the Host-Bacteria Interface: Host Defense or Bacterial Offense. *Trends Microbiol* 2019; 27 (3): 206-218.
8. Liu S, da Cunha AP, Rezende RM, et al. The Host Shapes the Gut Microbiota via Fecal MicroRNA. *Cell Host Microbe* 2016; 19 (1): 32-43.
9. Kao D, Roach B, Silva M, et al. Effect of Oral Capsule-Vs Colonoscopy-Delivered Fecal Microbiota Transplantation on Recurrent *Clostridium difficile* infection: A Randomised Clinical Trial. *JAMA* 2017; 318 (20): 1985-1993.
10. Lee C, Steiner T, Petrof EO, et al. Frozen vs Fresh Fecal Microbiota Transplantation and Clinical Resolution of Diarrhea in Patients With Recurrent *Clostridium difficile* Infection: A Randomized Clinical Trial. *JAMA* 2016; 315 (2): 142-9.
11. Seekatz AM, Theriot CM, Molloy CT, et al. Fecal Microbiota Transplantation Eliminates *Clostridium difficile* in a Murine Model of Relapsing Disease. Infect Immun 2015; 83 (10):3838-46.
12. Theriot CM, Koumpouras CC, Carlson PE, et al. Cefoperazone-treated mice as an experimental platform to assess differential virulence of *Clostridium difficile* strains. Gut Microbes 2011;2 (6):326-34.
13. Hirota SA, Iablokov V, Tulk SE, et al. Intrarectal instillation of *Clostridium difficile* toxin A triggers colonic inflammation and tissue damage: development of a novel and efficient mouse model of *Clostridium difficile* toxin exposure. Infect Immun 2012; 80(12):4474-84.

14. Polytarchou C, Oikonomopoulos A, Mahurkar S, et al. Assessment of Circulating MicroRNAs for the Diagnosis and Disease Activity Evaluation in Patients with Ulcerative Colitis by Using the Nanostring Technology. *Inflamm Bowel Dis* 2015; 21 (11): 2533-9.
15. Gu Z, Eils R, Schlesner M. Complex heatmaps reveal patterns and correlations in multidimensional genomic data. *Bioinformatics* 2016; 32 (18): 2847-9.
16. Ofir M, Hacohen D, Ginsberg D. MiR-15 and miR-16 are direct transcriptional targets of E2F1 that limit E2F-induced proliferation by targeting cyclin E. Mol Cancer Res. 2011 Apr;9(4):440-7. doi: 10.1158/1541-7786.MCR-10-0344.
17. Hassan MQ, Gordon JA, Beloti MM, Croce CM, van Wijnen AJ, Stein JL, Stein GS, Lian JB. A network connecting Runx2, SATB2, and the miR-23a~27a~24-2 cluster regulates the osteoblast differentiation program. Proc Natl Acad Sci U S A. 2010 Nov 16;107(46):19879-84. doi: 10.1073/pnas.1007698107.
18. Hu T, Chong Y, Cai B, et al. DNA methyltransferase 1-mediated CpG methylation of the miR-150-5p promoter contributes to fibroblast growth factor receptor 1-driven leukemogenesis. J Biol Chem. 2019 Nov 29;294(48):18122-18130. doi: 10.1074/jbc.RA119.010144.
19. Oikonomopoulos A, Polytarchou C, Joshi S, et al. Identification of Circulating MicroRNA Signatures in Crohn's Disease Using the Nanostring nCounter Technology. Inflamm Bowel Dis 2016;22(9):2063-9.
20. Chen G, Feng Y, Li X, et al. Post-transcriptional Gene Regulation in Colitis Associated Cancer. Front Genet 2019;10:585. doi: 10.3389/fgene.2019.00585. eCollection 2019.
21. Chandrasekaran R, Lacy DB. The role of toxins in *Clostridium difficile* infection. FEMS Microbiol Rev 2017; 41 (6): 723-750.
22. Di Bella S, Ascenzi P, Siarakas S, et al. *Clostridium difficile* Toxins A and B: Insights into Pathogenic Properties and Extraintestinal Effects. Toxins (Basel). 2016;8(5):134.

23. Nowarski R, Jackson R, Gagliani N., et al. Epithelial IL-18 Equilibrium Controls Barrier Function in Colitis. Cell 2015; 163: 1444-1456.

24. Yacyshyn MB, Reddy TN, Plageman LR, et al. Clostridium difficile recurrence is characterized by pro-inflammatory peripheral blood mononuclear cell (PBMC) phenotype. J Med Microbiol. 2014 Oct;63(Pt 10):1260-1273. doi: 10.1099/jmm.0.075382-0.

25. Yang Q, Li W, She H, et al. Stress induces p38 MAPK-mediated phosphorylation and inhibition of Drosha-dependent cell survival. Mol Cell 2015;57(4):721-734.

26. Farrow Ma, Chumbler NM, Lapierre LA, et al. Clostridium difficile Toxin B-induced Necrosis is mediated by the Host Epithleial Cell NADPH Oxidase Complex. Proc Natl Acad Sci USA 2013; 110: (46):18674-9.

27. Ye P, Liu Y, Chen C, et al. An mTORC1-Mdm2-Drosha axis for miRNA biogenesis in response to glucose- and amino acid-deprivation. Mol Cell 2015;57(4):708-720.

28. Wang X, Zhao X, Gao P, et al. c-Myc modulates microRNA processing via the transcriptional regulation of Drosha. Sci Rep 2013; 3:1942.

29. Bezerra Lima B, Faria Fonseca B, da Graça Amado N, Moreira Lima D, Albuquerque Ribeiro R, Garcia Abreu J, de Castro Brito GA. *Clostridium difficile* toxin A attenuates Wnt/β-catenin signaling in intestinal epithelial cells. Infect Immun 2014;82(7):2680-7.

30. Chen P, Tao L, Wang T, et al. Structural basis for recognition of frizzled proteins by Clostridium difficile toxin B. Science 2018;360(6389):664-669.

31. The Effects of Surface Layer Proteins Isolated from Clostridium difficile on TLR4 signalling- Kathy F. Kennedy M.Sc.

32. Jin F, Hu H, Xu M, et al. Serum microRNA Profiles Serve as Novel Biomarkers for Autoimmune Diseases. Front Immunol 2018; 9:2381. doi: 10.3389/fimmu.2018.02381.

33. Burrell C, Garavaglia F, Cribiu FM, Ercoli G, et al. Therapeutic faecal microbiota transplantation controls intestinal inflammation through IL10 secretion by immune cells. Nat Comm 2018; 9: 5184.

Figure Legends

Table 1. Participant baseline characteristics for discovery and replication cohorts.

Figure 1. Fecal Microbiota Transplantation (FMT) in patients with *C. difficile* infection regulates the levels of circulating miRNAs. *(A)* Heatmap representation of the significantly upregulated circulating miRNAs 4- and 12-weeks after FMT treatment compared to the screening time point (n = 42), as assessed by the nCounter Nanostring platform. *(B)* Representative box plots depicting the miRNAs with highest levels of detection. Box plots denote mean % change ± s.e.m., inner boxes represent mean, and error bars represent 95% confidence interval. Statistical significance of FMT effect on circulating miRNAs was determined by non-parametric longitudinal method followed by Wilcoxon signed-rank test for pairwise comparisons; $^{**}P < 0.01$, $^{***}P < 0.001$. *(C)* The overlapping top three miRNA-regulated pathways, as assessed by the Metacore network analysis software. *(D)* Validation of top 6 upregulated miRNAs in the replication cohort 2-

and 4-weeks after FMT as assessed by RT-qPCR. Fold changes and statistical significance in circulating levels of miRNAs was determined by OriginPro and Wilcoxon matched-pairs signed rank test; ***$P < 0.001$.

Figure 2. FMT reverses the effects of *C. difficile* on circulating and tissue miRNAs in a mouse model of recurrent CDI. Box plots depicting the changes in miRNA levels in *(A)* sera and *(B)* ceca from animals treated with FMT, infected with *C. difficile* (CDI), and infected with *C. difficile* and treated with FMT (CDI+FMT) compared to FMT donors. Box plots denote mean % change ± s.e.m., inner boxes represent mean, and error bars represent 95% confidence interval. miRNA levels were assessed by RT-qPCR and were normalised against *(A)* RNU1A1 and cel-miR-39 (spike-in) or *(B)* RNU5G and 5S rRNA, and compared to control (donor) samples, set as 100%. Statistical significance was determined by Student's *t*-test, *$P < 0.05$, **$P < 0.01$, ***$P < 0.001$ (compared to donor) and $^{\#}P < 0.05$, $^{\#\#}P < 0.01$, $^{\#\#\#}P < 0.001$ (compared to CDI).

Figure 3. Downregulation of miRNAs in mouse colonic tissues and human colonoids treated with *C. difficile* toxins. *(A)* Box plots depicting the changes in miRNA levels in colonic tissues from animals treated with TcdB and combination of TcdA with TcdB, compared to HBSS-treated controls (Vehicle). Box plots denote mean % change ± s.e.m., inner boxes represent mean, and error bars represent 95% confidence interval. miRNA levels were assessed by RT-qPCR, were normalized against RNU5G and 5S rRNA, and compared to control samples, set as 100%. Changes in miRNA levels *(B)* 30 min and *(C)* 6h in colonoids treated with TcdA or TcdB, compared to DMEM-treated controls (Vehicle). miRNA levels assessed by RT-qPCR, were normalized against RNU1A1 and 5S rRNA and are expressed as mean ± s.e.m. compared to control samples, set as 1. Statistical significance was determined by Student's *t*-test, *$P < 0.05$, **$P < 0.01$, ***$P < 0.001$.

Figure 4. *C. difficile* infection suppresses Drosha expression and miRNA processing. *(A)* Drosha mRNA and protein levels in ceca from animals treated with FMT, infected with *C. difficile* (CDI), infected with *C. difficile* and treated with FMT (CDI+FMT), compared to FMT donors. *(B)* Drosha mRNA levels in colonic tissues from animals treated with TcdB or combination of TcdA with TcdB, compared to controls (Vehicle). *(C)* Drosha mRNA and protein levels in colonoids treated with toxin A or toxin B, compared to DMEM-treated controls (Vehicle). *(D)* Drosha protein levels in NCM356 colonic epithelial cells upon knockdown of Drosha by means of siRNA (left) and treated with toxin B (right), compared to non-targeting siRNA (siControl) and DMEM-treated controls (Vehicle), respectively. *(E)* Pri-miRNA levels in NCM356 cells upon knockdown of Drosha (upper panel), and in colonoids treated with TcdA or TcdB (lower panel), compared to non-targeting siRNA (siControl) and DMEM-treated controls (Vehicle), respectively. mRNA and pri-miRNA levels assessed by RT-qPCR were normalized against beta-Actin and GAPDH and are expressed as mean ± s.e.m. compared to control samples, set as 1. Drosha protein levels were assessed by immunoblot analysis. alpha-Tubulin was used as the loading control. Statistical significance was determined by Student's *t*-test, $*P < 0.05$, $**P < 0.01$ and $^{\#\#}P < 0.01$ (compared to CDI). *(E)* Lower right panel, schematic representation of the proposed model on microRNA regulation by *C. difficile* infection.

Figure 5. Effects of Fecal Microbiota Transplantation (FMT)-regulated miRNAs in patients with *C. difficile* infection, on circulating proteins. *(A)* Effects of miR-26b-5p, miR-23a-3p, miR-150-5p and miR-28-5p overexpression on the levels of FGF21, IL12B, IL18 and TNFRSF9 mRNAs, respectively, in colonic epithelial cells. Gene expression data normalized against beta-Actin and GAPDH are expressed as mean ± s.e.m. compared to miR-C transfected cells, set as 1. *(B)* Effects of miR-26b-5p, miR-23a-3p, miR-150-5p and miR-28-5p on the activity of IL12B, IL18 and FGF21 mRNA 3'UTRs, as assessed by luciferase reporter assays. 3'UTR sequences were cloned in a reporter vector downstream of the *Renilla* Luciferase gene. The reporter vector was transfected in colonic epithelial cells and luciferase activity was measured 24 hours after the

overexpression of the respective miRNAs in the same cells. Direct targeting of the 3'UTR by the miRNA was validated by assays employing deletion mutants (DM) of the respective miRNA target sequences. *Renilla* Luciferase activity was normalized against the activity of the *Firefly* Luciferase gene, expressed by the same vector. miR-C (cel-miR-39-3p), a non-targeting miRNA was used as negative control. *(C) C. difficile* infection effect on the levels of circulating miR-26b-5p, miR-23a-3p, miR-150-5p and miR-28-5p in patients. The levels of serum miRNAs in *C. difficile* patients compared to healthy controls (n = 42), as assessed by the nCounter Nanostring platform. Box plots denote mean % change ± s.e.m., inner boxes represent mean, and error bars represent 95% confidence interval. *(D)* Effects of IL-18 on toxin-mediated cell growth inhibition. NCM356 cell growth was monitored in real-time as % of confluence (IncuCyte). *(E)* Effects of IL-18 on TcdB-mediated cell growth inhibition. NCM460 cell survival was assessed by measuring metabolically active cells (Cell-Titer Glo) and is expressed as mean ± s.e.m. compared to untreated cells, set as 100%. Statistical significance was determined by Student's *t*-test, $*P < 0.05$, $**P < 0.01$, $***P < 0.001$, compared to miR-C *(A* and *B),* healthy controls *(C)* and TcdB alone *(D* and *E)*, and $^{\#\#}P < 0.01$, $^{\#\#\#}P < 0.001$, compared to wild type 3'UTRs).

Figure 6. Functional effects of Fecal Microbiota Transplantation (FMT)-regulated miRNAs on colonic epithelial cells. *(A)* Effects of FMT-regulated miRNAs overexpression on TcdB-mediated cell growth inhibition. NCM356 cell survival was assessed by measuring metabolically active cells (Cell-Titer Glo) and is expressed as mean ± s.e.m. compared to miR-C transfected cells, set as 100%. *(B)* Effects of miR-23a-3p and miR-150-5p overexpression on TcdB-mediated NCM356 cell growth inhibition. Cells were monitored in real-time as % of confluence (IncuCyte). *(C)* Effects of miR-23a-3p and miR-150-5p overexpression on TcdB-mediated NCM460 cell growth inhibition. Cell survival was assessed by measuring metabolically active cells (Cell-Titer Glo) and is expressed as mean ± s.e.m. compared to miR-C transfected cells, set as 100%. *(D)* Effects of miR-23a-3p and miR-150-5p overexpression on TcdB-induced cell apoptosis. NCM356 cell

apoptosis was monitored in real-time as activated caspase3/7 fluorescence (IncuCyte). *(E)* Effects of miR-23a-3p and miR-150-5p overexpression on TcdB-mediated cytoskeleton rearrangements. NCM356 cytoskeleton organisation was studied by fluorescence microscopy after phalloidin staining. miR-C (cel-miR-39-3p), a non-targeting miRNA, was used as negative control. Statistical significance was determined by Student's *t*-test, $*P < 0.05$, $**P < 0.01$.

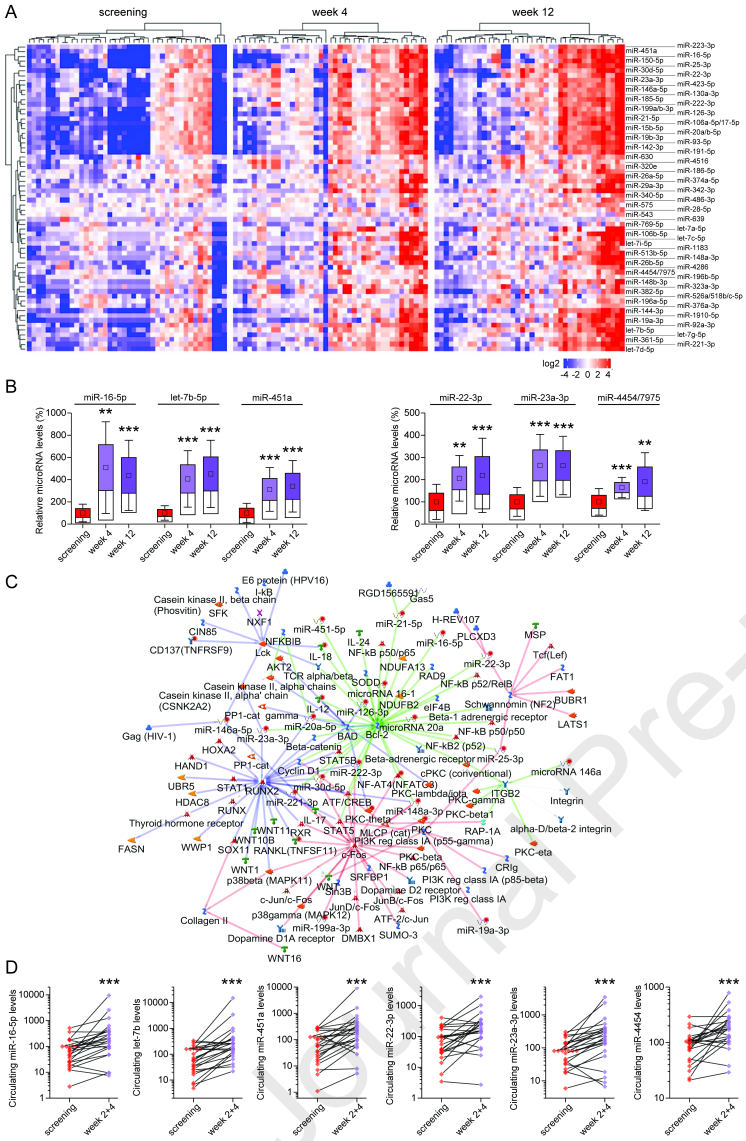

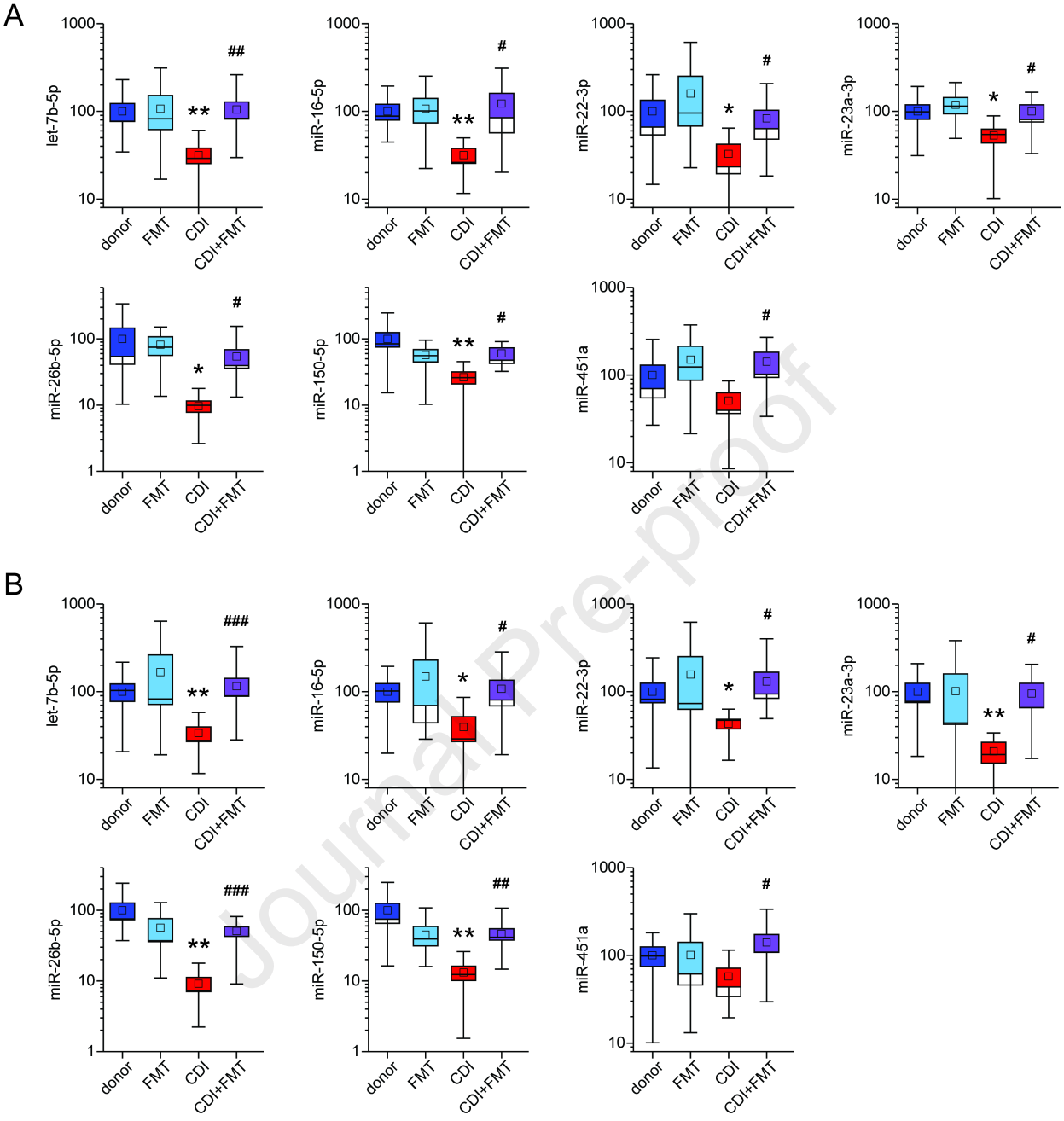

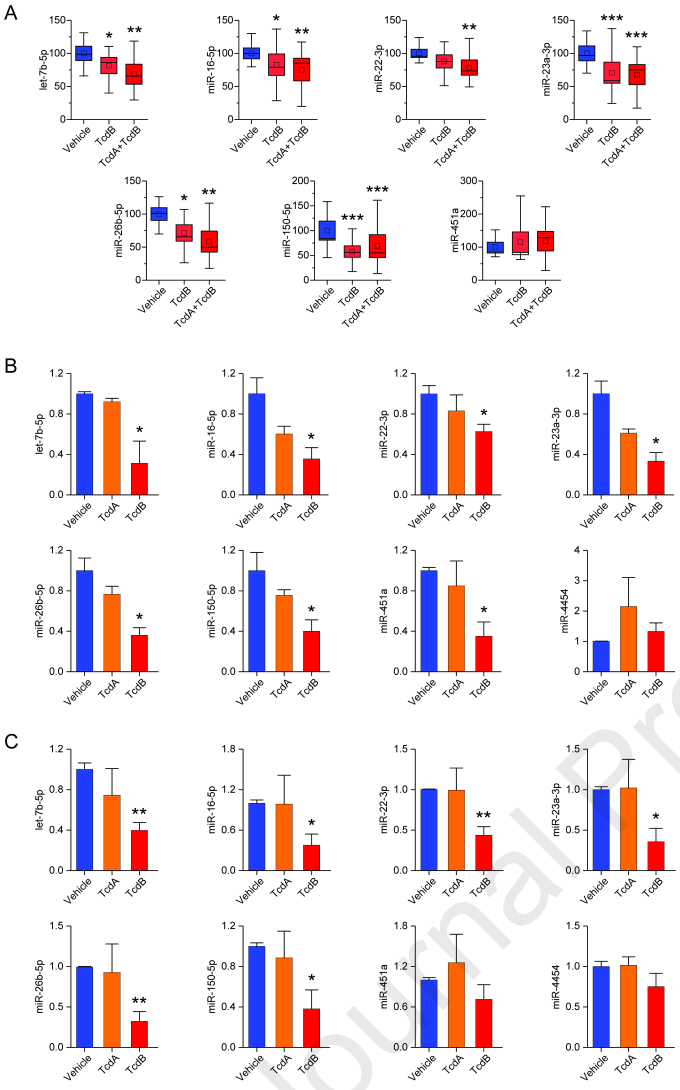

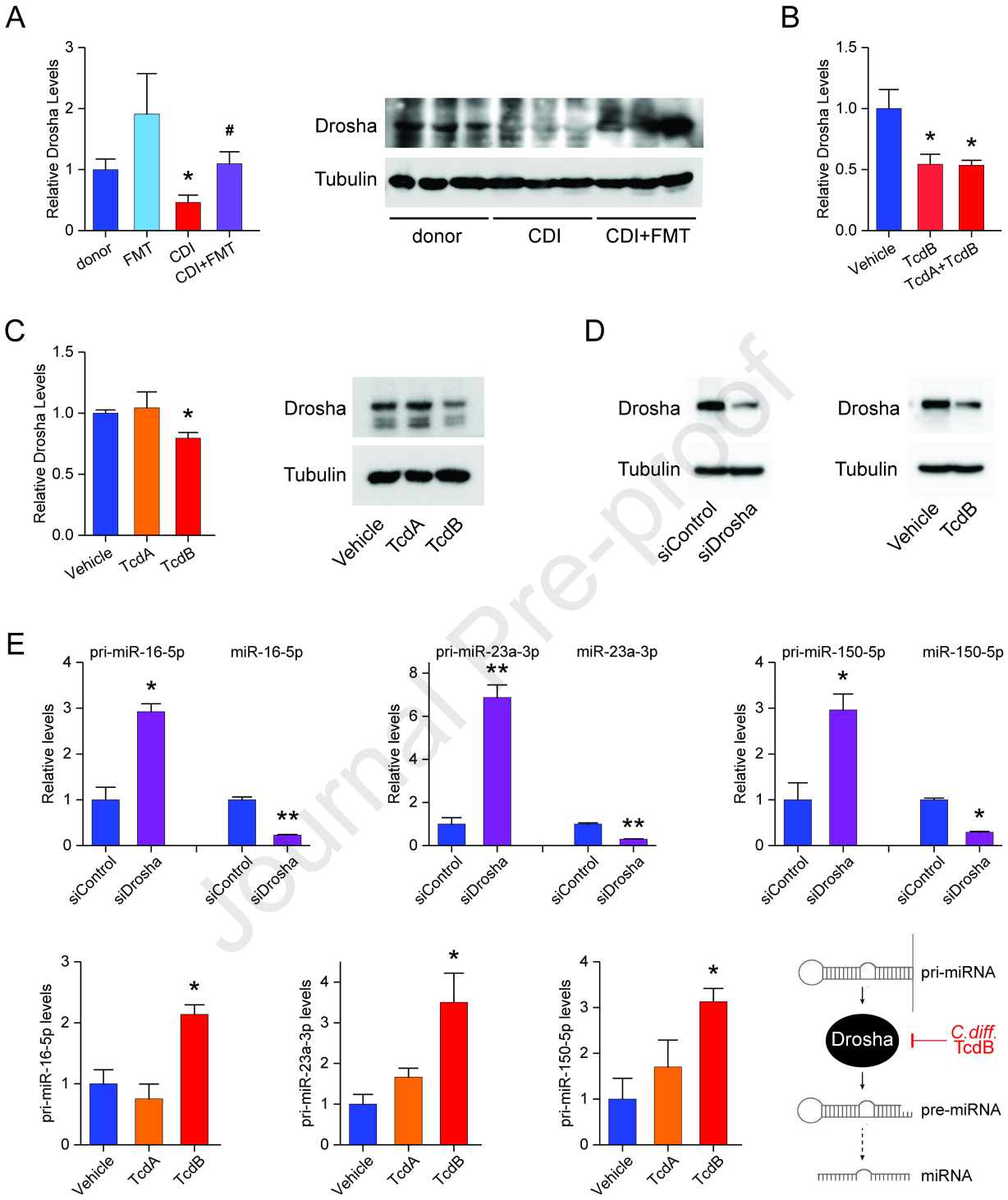

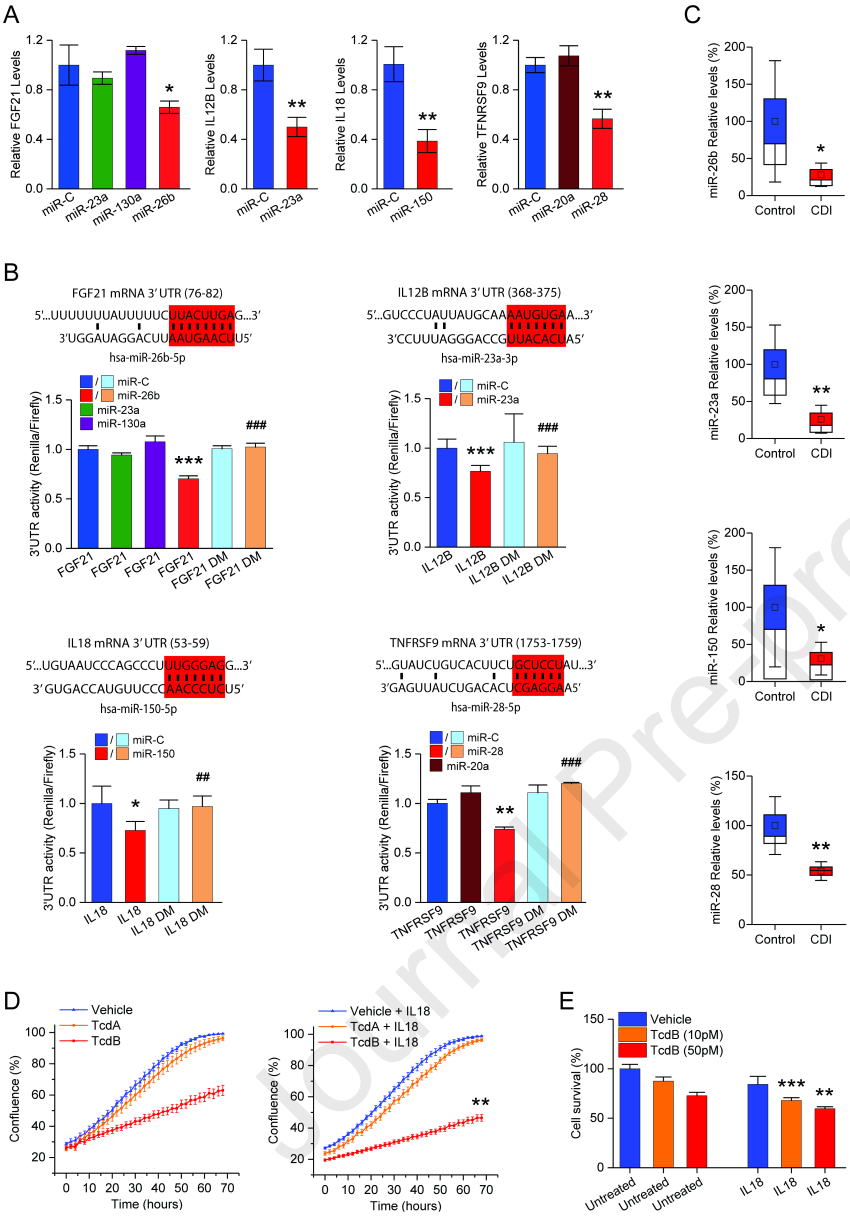

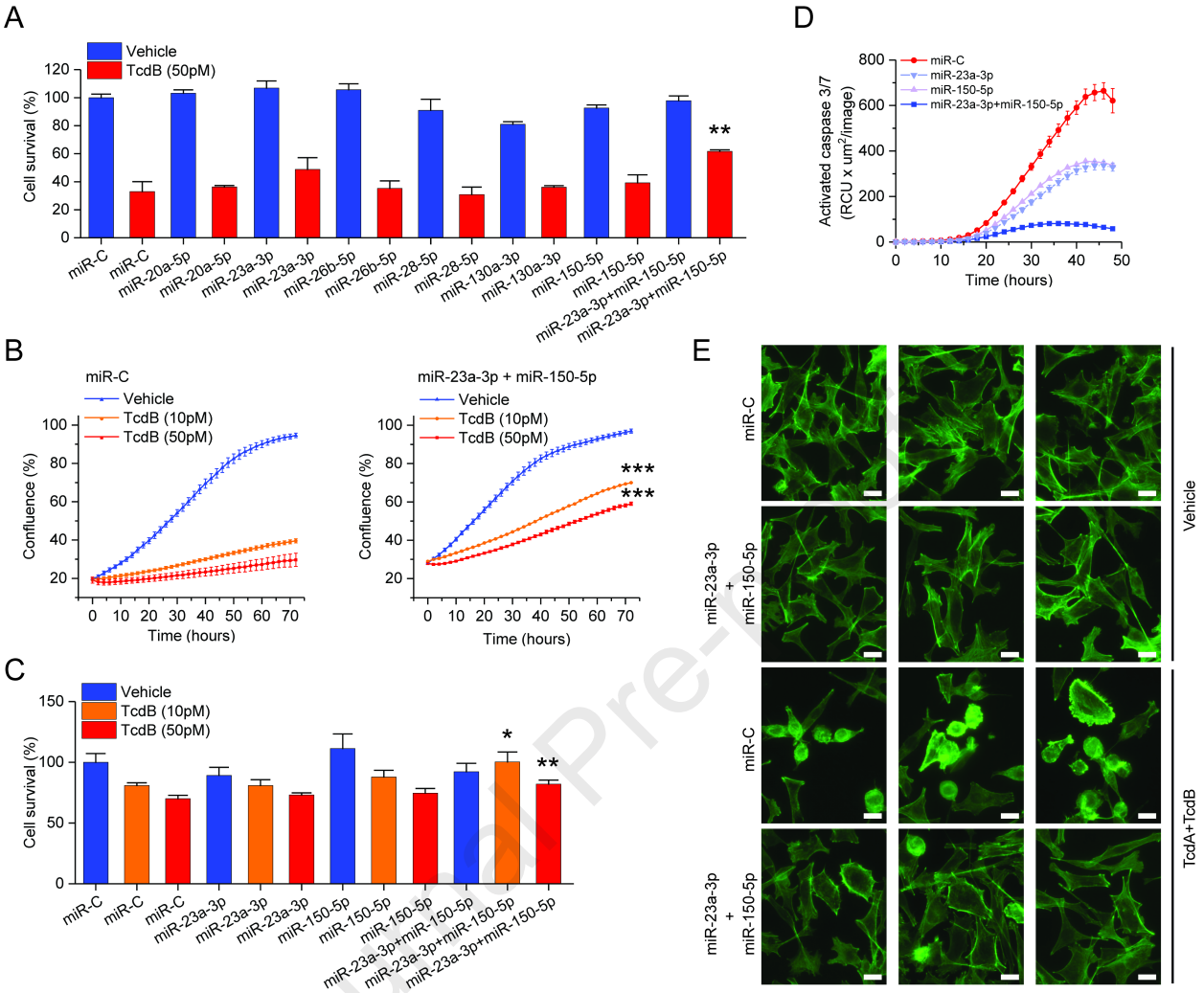

	Discovery Cohort - NCT02254811			**Replication Cohort - NCT01398969**		
	Capsule (n = 25)	**Colonoscopy (n = 17)**	***P* value**	**Fresh (n = 11)**	**Frozen (n = 13)**	***P* value**
Age, mean (SD), y	59.0 (19.7)	56.4 (18.7)	0.6624	74.3 (14.1)	71.6 (18.6)	0.7363
Females, No. (%)	21 (84.0%)	9 (52.9%)	0.0659	4 (36.4%)	9 (69.2%)	0.2305
Charlson comorbodity index, median	3 (2-5)	3 (0-4)	0.4353			
Immunosuppressed patients, No. (%)	2 (8.0%)	3 (17.6%)	0.6439	3 (27.3%)	1 (7.7%)	0.4637
Use of immune modulator, No. (%)						
Costicosteroid	0 (0%)	1 (5.9%)	0.8443			
Immunosuppresant	1 (4.0%)	1 (5.9%)	1	4 (36.4%)	3 (23.1%)	0.7926
Biologic	2 (8.0%)	1 (5.9%)	1	5 (45.5%)	4 (30.8%)	0.751
Body mass index (BMI), mean (SD)	25.3 (6.6)	27.0 (4.1)	0.3113			
Inpatient status at screening, No. (%)	3 (12%)	0 (0%)	0.3833	7 (63.6%)	6 (46.2%)	0.6561
PPI use prior to FMT, No. (%)	4 (16%)	1 (5.9%)	6111	5 45.5%)	5 (38.5%)	1
No. of RCDI episodes prior to FMT; median	3 (3-4)	3 (3-4)	0.3893	3 (2.5-4.0)	3 (3-4)	0.4641
Duration of RCDI prior to FMT, median	65 (49-96)	70 (57-135)	0.2648			
No. of CDI related hospital admissions, median	1 (0-2)	0 (0--0)	0.0057			
IBD, No. (%)						
Ulcerative colitis	2 (8.3%)	3 (1.8%)	0.6439			
Crohn's	2 (8.3%)	1 (5.9%)	1	2 (18.2%)	2 (15.4%)	1
Hemoglobin (g/dL), median	137 (129-144)	138 (132-144)	0.6079			
WBC (10^9/L), median	8 (6.8-8.6)	6.5 (5.1-6.9)	0.0143	15.30 (8.35-21.70)	8.9 (6.7-12.6)	0.2212
Albumin (g/L), median	40.5 (38.8-43.3)	40 (38-42)	0.5857	31 (28-34)	30 (24-34)	0.8557
CRP (mg/L), median	1.9 (0.9-5.8)	6.2 (1.3-10.2)	0.244			
Creatinine (mg/dL), median	70 (58.75-76)	70 (59-84)	0.7404	88 (69.5-127)	85 (64-128)	0.6849

Table 1. Participant baseline characteristics for the discovery and replication cohorts			

WHAT YOU NEED TO KNOW

BACKGROUND AND CONTEXT

Fecal microbiota transplantation (FMT) is highly effective at preventing recurrent *Clostridioides difficile* infection (rCDI). However, the mechanisms of action remain largely unknown. MicroRNAs (miRNAs), short non-coding RNA sequences which bind to complementary sequences of mRNA and can regulate gene expression, may be a potential mechanism by which commensal microbiota communicate with the human host.

NEW FINDINGS

We identified several significant alterations in circulating miRNAs following successful FMT treatment in 2 independent rCDI patient cohorts. miRNA signatures were validated in animal models and human colonoids. We further demonstrate that FMT-regulated miRNAs regulate cell properties and target IL-12B, IL-18, FGF21 and TNFRSF9, integral in pathways linking to inflammation, autoimmunity and cancer.

LIMITATIONS

Deeper characterization of the epitranscriptome in FMT is required.

IMPACT

These results describe a new mechanism of action of FMT against rCDI and provide potential new therapeutic targets for conditions associated with intestinal dysbiosis.

LAY SUMMARY

Successful fecal microbiota transplantation for recurrent *Clostridioides difficile* infection associates with increased expression of specific microRNAs in blood and colonic tissues. These microRNAs target inflammatory proteins and can protect gut barrier from damage from *C. difficile* toxins.

Supplementary Methods

RT-qPCR for miRNAs

For RT-qPCR miRNA analysis, reverse transcription was performed using miRCURY LNA RT Kit (339340) and quantitative polymerase chain reaction (qPCR) for hsa-let-7b-5p (miRCURY LNA primer set, YP00204750), hsa-miR-16-5p (YP00205702), hsa-miR-22-3p (YP00204606), hsa-miR-23a-3p (YP00204772), hsa-miR-26b-5p (YP00204772), hsa-miR-150-5p (YP00204772), hsa-miR-4454 (YP02114119), hsa-miR-451a (YP02119305), cel-miR-39-3p (YP00203952), RNU1A1 (YP00203909), RNU5G (YP00204772) and 5S rRNA (YP00203906) using miRCURY LNA SYBR Green PCR Kit (339346, Qiagen, Hilden, Germany) on CFX384 real-time PCR detection system (Bio-Rad, Hercules, California, USA). The qPCR conditions applied were 95°C for 10 min, and 40 cycles of 95°C for 10 s and 60°C for 1 min, followed by melting curve analysis. qPCR reactions were performed in quadruplicates and cel-miR-39-3p (spike-in), RNU5G, RNUA1 and 5S rRNA were used as reference genes.

Cell culture and transfection

Human NCM356 colonic epithelial cell line (Incell, San Antonio, Texas, USA) and peripheral blood mononuclear cells (PBMC) were cultured in M3Base medium (M300F) and Roswell Park Memorial Institute medium 1460 (RPMI-1460), respectively, supplemented with 10% fetal bovine serum (FBS) (10270-106; Life Technologies, Carlsbad, California, USA) and 1% Penicillin-Streptomycin (15070-063) in a humidified incubator at 37°C with 5% CO_2. Treatment with cytokines was performed at the concentration of 50 ng/ml using recombinant human IL-12 p70 (Peprotech, 200-12H), IL-18/IL-1F4 (R&D, 9124-IL-010), FGF-21 (R&D, 2539-FG-025) or 4-1BB Ligand/TNFSF9 (R&D, 2295-4L-025). For transfections, cells were plated in 6-well tissue culture plates and transfected with hsa-miR-20a-5p (YM00472205),

hsa-miR-23a-3p (YM00470983), hsa-miR-26b-5p (YM00472485), hsa-miR-28-5p (YM00471553), hsa-miR-130a-3p (YM00472237), hsa-miR-150-5p (YM00470312) miRCURY LNA miRNA mimics, miRNA control (YM00479902, Qiagen) at a final concentration of 20nM or with siRNA against Drosha (Dharmacon, ON-TARGETplus Human DROSHA siRNA, SMARTPool, L-016996-00-0005) or the respective siControl (Dharmacon, ON-TARGETplus non-targeting control pool, D-001810-10-05) using Lipofectamine RNAiMAX (13778-150; Invitrogen, Carlsbad, CA, USA) according to manufacturer's instructions. PBMCs were treated with miRCURY LNA microRNA inhibitors (20nM) for hsa-miR-150-5p (YI04101205), hsa-miR-26b-5p (YI04104759) or negative inhibitor control (YI00199007, Qiagen) without transfection reagent. Cells were collected 24 h later for RNA extraction.

RNA extraction, RT-qPCR for genes

Tissues were homogenized in Trizol (15596026, Invitrogen) and total RNA was isolated according to established protocols. Total RNA from cell cultures was isolated using QIAshredder (79656) and RNeasy Plus Mini Kit (74136, Qiagen) according to manufacturer's instructions. Reverse transcription was performed using iScript Reverse Transcription Supermix (170-8841). cDNAs were subjected to quantitative polymerase chain reaction (qPCR) using iTaq Universal SYBR Green Supermix (172-5124, Bio-Rad) on a CFX384 real-time PCR detection system (Bio-Rad) and the primers listed in Supplementary Table 1. The qPCR conditions were 95°C for 30 s, and 45 cycles of 95°C for 15 s, 55°C for 10 s and 72°C for 30 s, followed melting curve analysis. β-actin and GADPH were used as reference genes. Results are derived from 3 independent experiments performed in quadruplicates.

Immunoblot analysis

Tissues and colonoids were homogenized using RIPA cell lysis buffer (9806, Cell Signaling Technology) supplemented with protease inhibitors (04693132001, Roche). Western blots of electrophoresed (SDS-PAGE) cell lysates were probed with Ago2 (2897), Drosha (3364, Cell Signaling Technology), Dicer (sc-136981, Santa Cruz) and alpha-Tubulin (T5168, Sigma) monoclonal antibodies, following standard procedures.

Construction of 3'UTR reporter vectors

miRNA target predictions were performed using the TargetScan 7.2 software [3]. All 64 miRNAs found to be induced by FMT were screened against the 3'UTR of FGF21, IL-12B, IL-18 and TNFRSF9. The 3'UTR sequences of FGF21, IL-12B, IL-18 and TNFRSF9 were amplified using Q5 High-Fidelity DNA Polymerase (M0491; NEB, Ipswich, Massachusetts, USA) according to the manufacturer's instructions, using the primers listed in Supplementary Table 2. The amplified 3'UTR sequences were cloned into psi-CHECK2 vector (C8021; Promega, Madison, Wisconsin, USA), downstream of the *Renilla Luciferase* gene. *Firefly Luciferase* gene expressed by this vector independently of the 3'UTR sequences was used as reference. The 3'UTRs at the corresponding miRNA target sequence (miR-26b for FGF21; miR-23a for IL-12B; miR-150 for IL-18; miR-28 for TNFRSF9) were mutated (deletion mutants) using the QuikChange II site-directed mutagenesis kit (200524; Aligent Technologies, Santa Clara, California, USA) according to the manufacturer's instructions. Primers used for mutagenesis are listed in Supplementary Table 3. Cloned sequences and mutations were verified by DNA sequencing.

3'UTR reporter assays

NCM356 cells were plated in a 6-well plate and transfected with the 3'UTR reporter vectors using Lipofectamine 3000 (L3000-008; Invitrogen, Carlsbad, California, USA). Cells were transfected, 24 h later, with the respective microRNA mimic or the control (Qiagen, Hilden,

Germany) by using Lipofectamine RNAiMAX (13778-150). 20,000 cells/well were plated in Nunclon Delta Surface 96-well plate (136101; Thermo Scientific, Waltham, Massachusetts, USA) and Luciferase activity (luminescence) was measured using the Dual-Luciferase Reporter Assay kit (E1980; Promega, Madison, Wisconsin, USA), on a Cytation 3 multi-mode reader (BioTek, Winooski, Vermont, USA), according to the manufacturer's instructions. *Renilla* Luciferase activity was normalized against *Firefly* Luciferase activity per well. Results are derived from 3 independent experiments performed in quadruplicates.

Luminescence cell viability assay

Cells were transfected with the respective miRNAs and plated in quadruplicates in 96-well plate ($25x10^3$ cells/well). 48h following transfection, cells were treated with TcdA and/or TcdB (at the concentrations of 10 or 50 pM). In another set of experiments, 48h following transfection, the cells were treated with the respective cytokines (at at the concentration of 50ng/ml) and 30 min later TcdA and/or TcdB was added (at at the concentrations of 10 or 50 pM). Following treatment, growth was assessed at 48h using the CellTiter Glo Luminescence Cell Viability Assay (G7573, Promega) according to the manufacturer's instructions. Luminescence readings were acquired with CLARIOstar plate reader (BMG Labtech). Data were expressed as mean luminescence (arbitrary units) ± s.e.m. (control cells were set as 100%).

IncuCyte Live-Cell growth assay

Cells were transfected with the respective miRNAs and plated in quadruplicates in 96-well plate ($25x10^3$ cells/well). 48h following transfection, cells were treated with TcdA and/or TcdB (at the concentrations of 10 or 50 pM). In another set of experiments, 48h following transfection, the cells were treated with the respective cytokines (50ng/ml) and 30 min later TcdA and/or TcdB was added (10 or 50 pM). Following treatment, growth was assessed

using the IncuCyte Live-Cell analysis system, where images with 10X magnification were captured every 2 hours for total of 3 days and analysed. Data were expressed as mean % confluency ± s.e.m.

IncuCyte Live-Cell apoptosis assay

Cells were transfected with the respective miRNAs and plated in quadruplicates in 96-well plate ($25x10^3$ cells/well). 48h following transfection, cells were treated with TcdB (10 or 50 pM) and Incucyte Caspase-3/7 Red Dye for Apoptosis (Essen Bioscience, 4704) was added in the cells in a final concentration of 0.5 µM. Apoptosis was assessed using the IncuCyte Live-Cell analysis system, where images with 10X magnification were captured every 2 hours for total of 2 days and analysed. Data were expressed as mean % confluency ± s.e.m.

ApoTox-Glo Assay

Cells were transfected with the respective miRNAs and plated in quadruplicates in 96-well plate ($25x10^3$ cells/well). 48h following transfection, cells were treated with TcdB (10 or 50 pM). Cytotoxicity and cell survival was assessed at 2, 24 and 48h using the ApoTox-Glo Triplex Assay (Promega, G6320). Briefly, 20µl of Viability/Cytotoxicity Reagent containing both GF-AFC Substrate and bis-AAF-R110 Substrate, previously warmed at 37°C, was added per well. Contents were mixed briefly by orbital shaking at 300–500rpm for 30 seconds and incubated for 30 minutes at 37°C. Fluorescence was measured at 400Ex/505Em for cell viability and 485Ex/520Em for cell cytotoxicity, using the CLARIOstar plate reader (BMG Labtech).

Phalloidin actin staining

Cells were transfected with LNA miRNA mimics (20nM) for miR-23a-3p and miR-150-5p or cel-miR-39 as the control and plated in 8-well tissue culture coverslips (ibidi, 80826), pre-coated with 50 µg/ml collagen I (Life Technologies, A10483-01). 48h after transfection, cells

were treated with a combination of toxins A and B (10pM) for 4h. Following treatment, cells were fixed in 4% formaldehyde for 15 min at room temperature and rinsed (3x5min) with PBS. Permeabilization was achieved with 0.5% Triton X-100 in PBS, for 10 min at room temperature followed by 100mM glycine (in PBS, 0.1% Tween-20) for 2 min at room temperature and rinsed with PBS. Cells were incubated in Image-IT FX Signal Enhancer Ready Probes Reagent (Life Technologies, R37107) for 20 min at room temperature and then rinsed with 0.1% Triton X-100 in PBS, 20 min in blocking solution (PBS, 0.1%Triton X-100, 2% BSA) and rinsed with 0.1% Triton X-100 in PBS. Actin staining was performed with AlexaFluor 488 phalloidin (Life Technologies, R37110) and nuclei staining with NucBlue live ReadyProbes reagent (Life Technologies, R37605), in blocking solution, for 30 min at room temperature protected from light. Cells were rinsed once with 0.1% Triton X-100 in PBS and washed (3x5min) with PBS. Images were captured with a fully automated Zeiss AxioObserver Z1 inverted microscope equipped with AxioCam MRm high-resolution camera, using the AxioVision SE64 image acquisition software.

Supplementary Table 1. qPCR primers.

Gene	Forward	Tm (°C)	Reverse	Tm (°C)	Size (bp)
FGF21	5'-GGGAGTCAAGACATCCAGGT-3'	59	5'-TGTATCCGTCCTCAAGAAGCA-3'	60.8	116
IL18	5'-AGGAAATCGGCCTCTATTTG-3'	59.7	5'-CCATACCTCTAGGCTGGCTATC-3'	59.3	110
IL12B	5'-CATTGAGGTCATGGTGGATG-3'	59.8	5'-GGTGGGTCAGGTTTGATGAT-3'	59.6	93
AGO2	5'-GACACGAAAATCACCCACCC-3'	59.1	5'-GGACGTGATAGTGCGAAGG-3'	58	94
DICER1	5'-CTGCAAATGTACCCCGTTCC-3'	59.2	5'-GTGACTCTGACCTTCCCGTC-3'	59.8	106
DROSHA	5'-AGGACAGAAGGAAAAGAGCCA-3'	58.9	5'-ACAGTGTAGGTTCGGGCATG-3'	60	83
TNFRSF9	5'-CTGCCGATTTCCAGAAGAAG-3'	59.5	5'-GAAAGCTGTGATAGCGGATGA-3'	60.4	120
pri-miR-16-5p	5'-GCACGTAAATATTGGCGTTAAG-3'	56.5	5'-CACAACTGTAGAGTATGGTCAACCT-3'	61.3	88
pri-miR-23a-3p	5'-ATCACATTGCCAGGGATTTC-3'	55.2	5'-AGCTAAGCCCTGCTCCTCAG-3'	61.4	118
Actin	5'-CCCAGCACAATGAAGATCAA-3'	59.6	5'-ACATCTGCTGGAAGGTGGAC-3'	60.1	103
GAPDH	5'-ATGTTCGTCATGGGTGTGAA-3'	59.8	5'-GGTGCTAAGCAGTTGGTGGT-3'	60.2	89
pri-miR-150-5p	5'- GGGCTCAGACCCTGGTACA-3'	61	5'- GAGTACAGGGAGGGGAGGTC-3'	63.4	109
mAgo2	5'-CCACCCCACTGAGTTTGACT-3'	59.5	5'-TTGTCATCCCAAAGCACGTG-3'	59.1	93
mDicer1	5'-TCTGCAGGCTTTTACACACG-3'	58.8	5'-ACAGCCACAGTGTAGGTTCT-3'	58.6	88
mDrosha	5'-GGACAGAAGGGAAAGAGCCT-3'	59	5'-CCAAAATCGCATCTCCCAGG-3'	59	89
mActin	5'-CCAACCGTGAAAAGATGACC-3'	60.4	5'-CCATCACAATGCCTGTGGTA-3'	60.4	120
mGAPDH	5'-GTGTTTCCTCGTCCCGTAGA-3'	60.1	5'-AATCTCCACTTTGCCACTGC-3'	60.3	108

Supplementary Table 2. 3'UTR cloning primers.

Gene	Forward	Tm (°C)	Reverse	Tm (°C)
FGF21	5'-CT**CTCGAG** GCCAGAGGCTGTTTACTATGA-3'	57.1	5'-GC**GCGGCCGC** TCCTCCTCTGGAACTCTTTATTATC-3'	58.4
IL18	5'-CT**CTCGAG** GAGGATGAATTGGGGGATAGA-3'	59.8	5'-GC**GCGGCCGC** AAACATAAAAATTCAGACAGTTCACA-3'	58.7
IL12B	5'-CT**CTCGAG** TGATCCAGGATGAAAATTTGG-3'	60.1	5'-GC**GCGGCCGC** GAAGAGTTTTTATTAGTTCAGCCTCA-3'	58.3
TNFRSF9	5'-CT**CTCGAG** CTGCCGATTTCCAGAAGAAG-3'	68	5'-GC**GCGGCCGC** GAGGGTAGCAAGGATGTGGA-3'	76

Supplementary Table 3. Mutagenesis Primers.

Gene	Sense	Tm (°C)	Antisense	Tm (°C)
FGF21	5'-TCTGGAACTCTTTATTATCT CGTAAGAAAAATAAAAAAATAAAT -3'	62.9	5'-ATTTATTTTTTTATTTTTC TTACGAGATAATAAAGAGTTCCAGA-3'	62.9

IL18	5’-GTAATCCCAGCCCTTGG CTGAGGCGG-3’	71.1	5’-CCGCCTCAGCCAAGGG CTGGGATTAC-3’	71.1
IL12B	5’-TGTCAGTACAAATAAAATTA AATTTGCATAATAGGGACTGATCC-3’	66.6	5’-GGATCAGTCCCTATTAT GCAAATTTAATTTTATTTGTACTGACA-3’	66.6
TNFRSF9	5'-GTTATAGTAGAACCAACTAA AAGCAGAAGTGACAGATACCCA-3'	78.7	5'-TGGGTATCTGTCACTTCT GCTTTTAGTTGGTTCTACTATAAC-3'	78.7

References

1. Polytarchou, C. et al. *Inflamm Bowel Dis* 2015; 21: 2533-9

2. Gu, Z. et al. *Bioinformatics* 2016; 32: 2847-9

3. Agarwal, V. et al. eLife 2015; 4: e05005

SUPPLEMENTARY INFORMATION

Supplementary Data

Supplementary Figure 1.

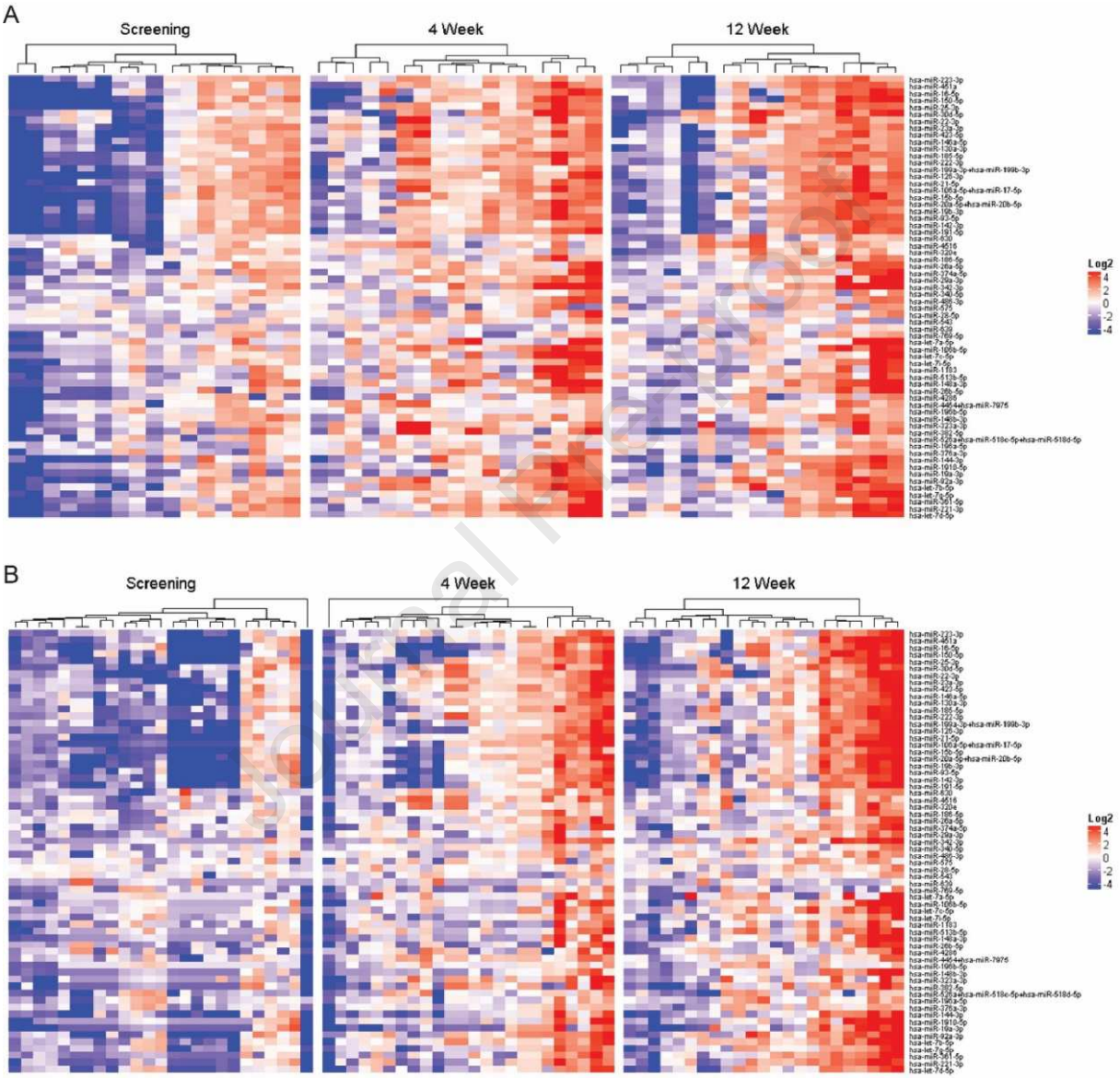

Figure S1. Fecal Microbiota Transplantation (FMT) delivered by capsule and colonoscopy to patients with recurrent *C. difficile* infection regulates the levels of circulating miRNAs. Heatmap representation of the upregulated circulating miRNAs 4 and 12 weeks after FMT treatment compared to the screening time point, as assessed by the nCounter Nanostring platform in recipients of *(A)* colonoscopy and *(B)* pill FMT.

Supplementary Figure 2.

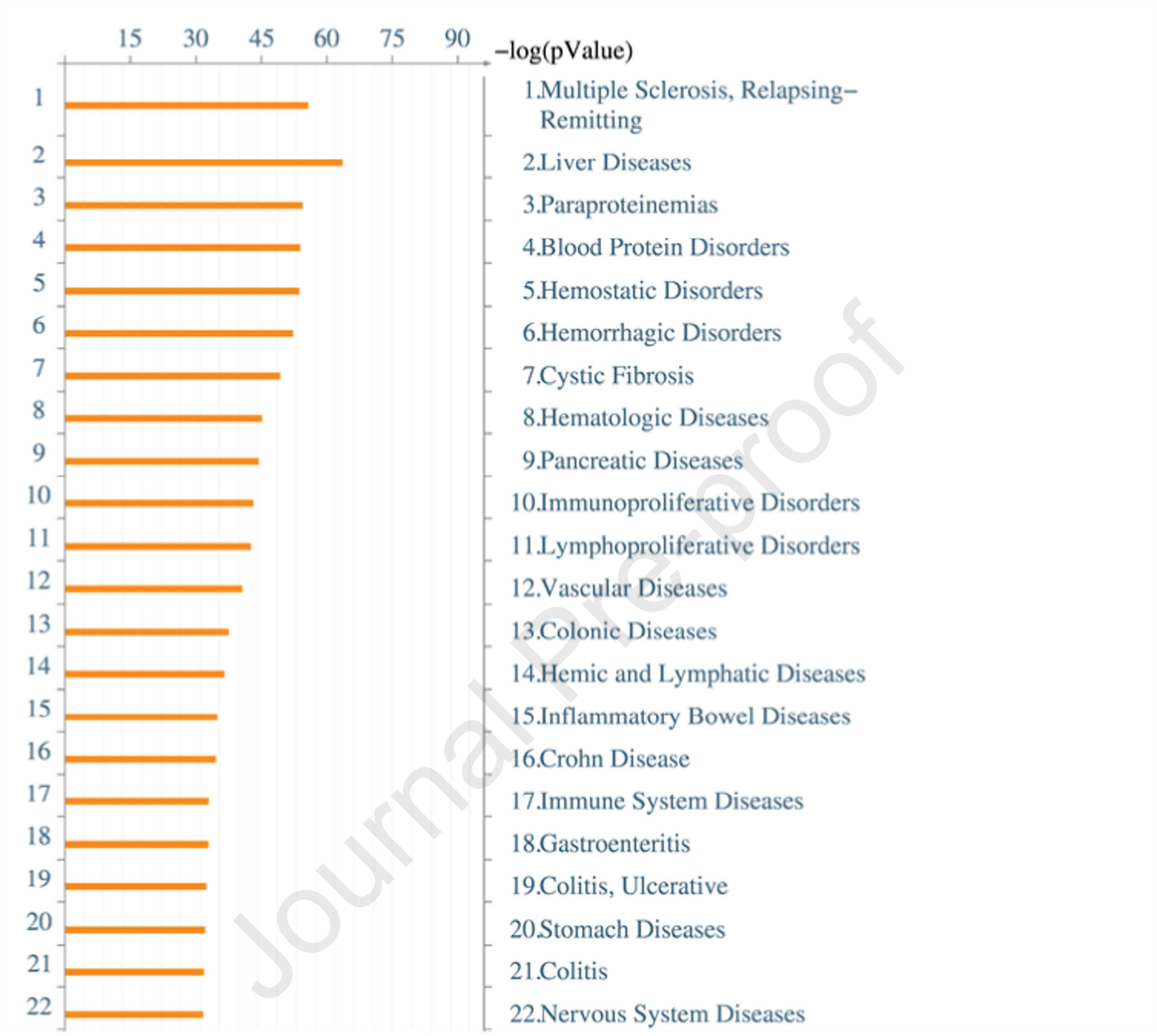

Fig S2. Circulating miRNAs changing after FMT treatment link with other pathologies. Potential applicability of FMT in other pathologies based on miRNA signatures. Analysis performed using the Metacore pathway analysis software.

Supplementary Figure 3.

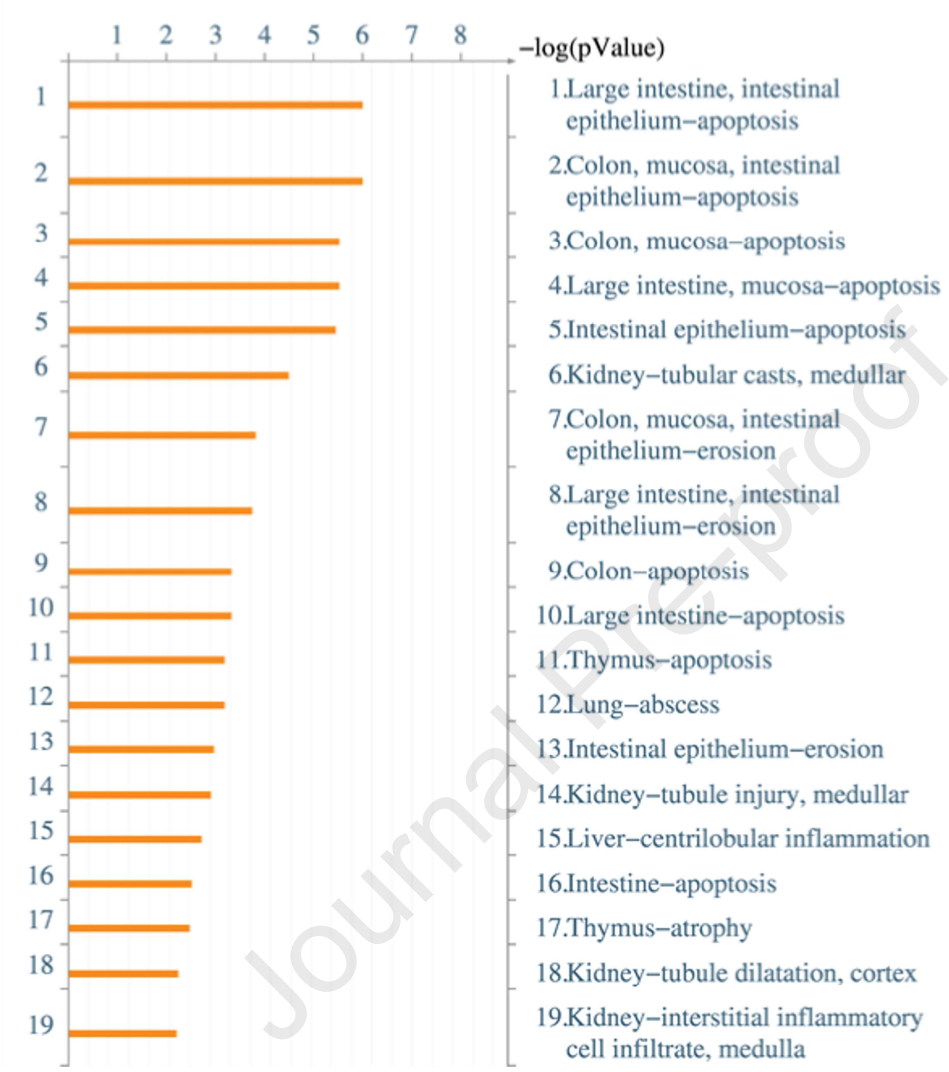

Fig S3. FMT-regulated miRNAs may provide mechanistic insights into FMT therapeutic applications. Circulating miRNAs changing after FMT associate with cell/tissue properties. Analysis performed using the Metacore pathway analysis software.

Supplementary Figure 4.

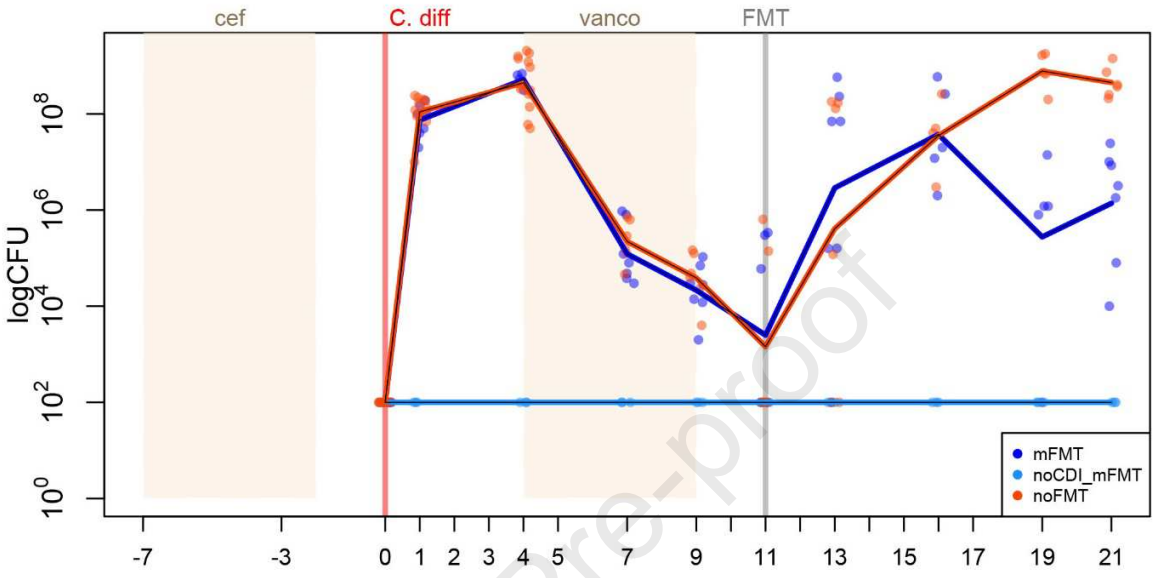

Fig S4. *C. difficile* load in animals infected with *C. difficile* strain 630 and treated with FMT. The *C. difficile* load, throughout the experiment, was assessed in individual fecal samples on taurocholate cycloserine cefoxitin fructose agar under anaerobic conditions after overnight incubation and is expressed as colony-forming unit/mL.

Supplementary Figure 5.

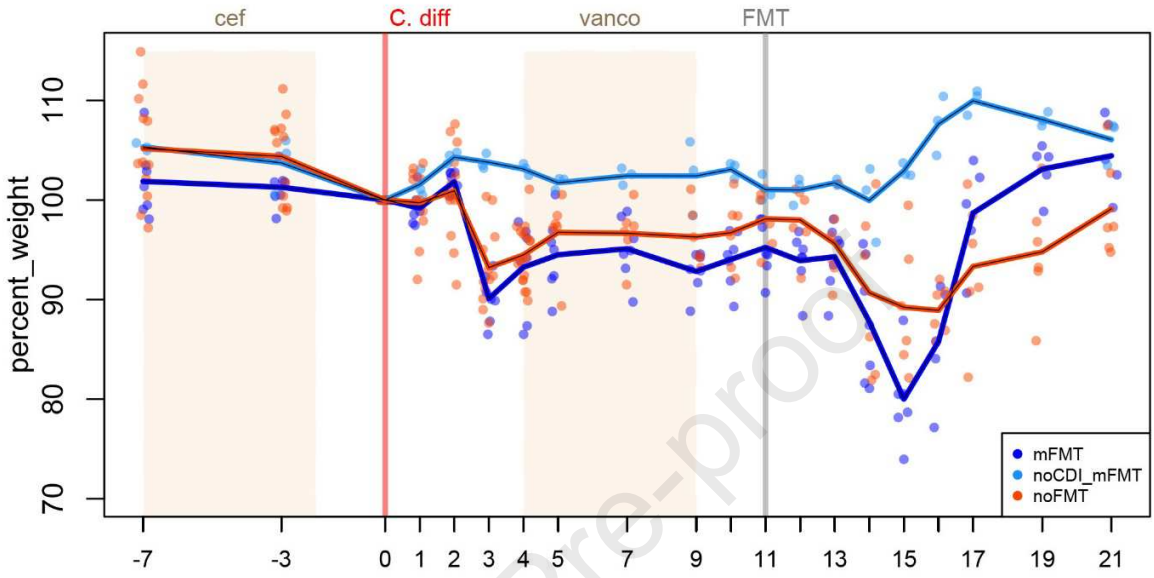

Fig S5. Body weights of animals infected with *C. difficile* strain 630 and treated with FMT. Body weight was assessed for individual animals and is expressed as % change compared to time point 0 (day of infection) per experimental group.

Supplementary Figure 6.

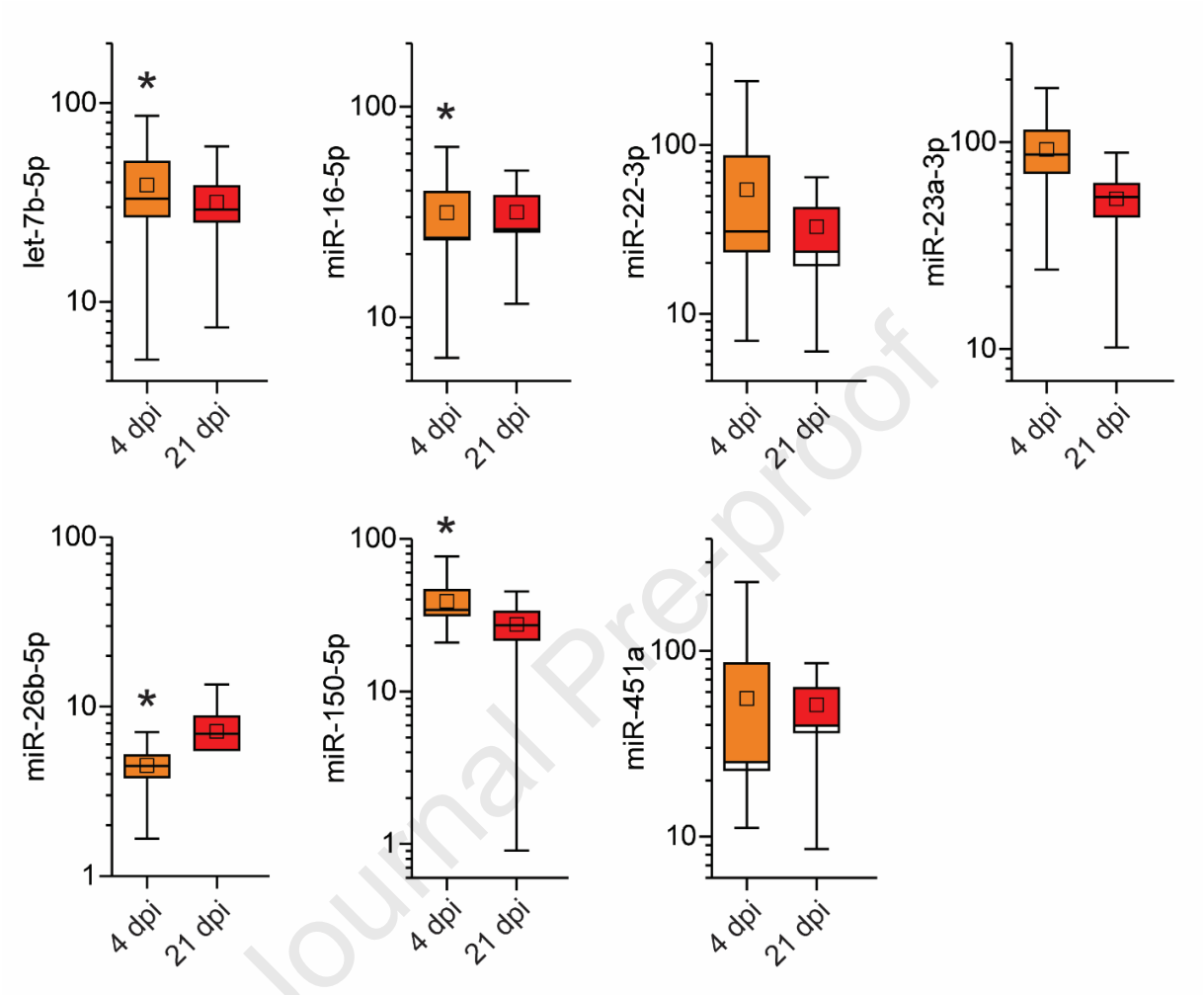

Fig S6. Effects of *C. difficile* strain 630 on circulating miRNAs in the mouse model of recurrent CDI. Box plots depicting the changes in miRNA levels in sera from mice infected with *C. difficile*, 4- and 21-days post infection (dpi). Box plots denote mean % change ± s.e.m., inner boxes represent mean, and error bars represent 95% confidence interval. miRNA levels were assessed by RT-qPCR normalized against RNU1A1 and cel-miR-39 (spike-in), and compared to control group (FMT donors), set as 100%. Statistical significance was determined by Student's *t*-test, *$P < 0.05$ (compared to donor). The 21 dpi data (statistical analysis provided in Fig. 2A) are included for comparisons.

Supplementary Figure 7.

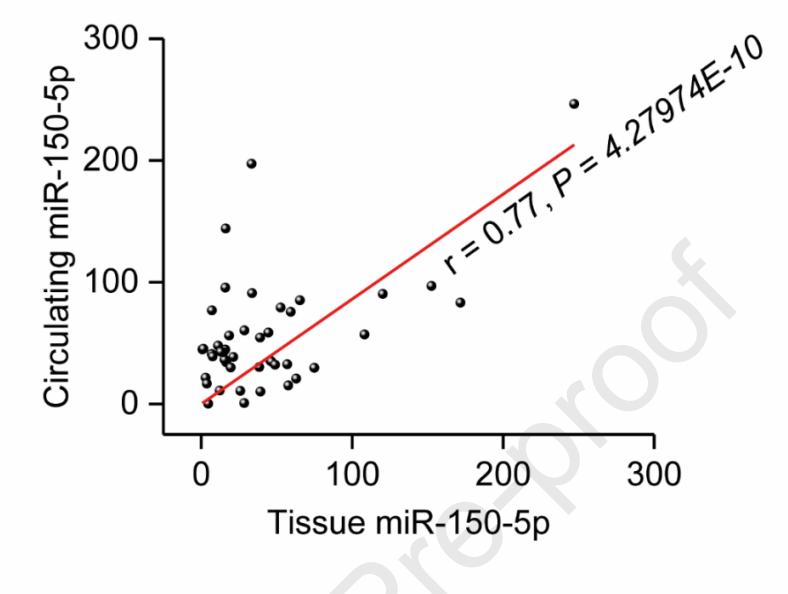

microRNA	Pearson's r	*P value*
miR-150-5p	0.77	*4.27974E-10*
miR-22-3p	0.65	*1.66563E-6*
miR-23a-3p	0.58	*3.69214E-5*
miR-451a	0.56	*6.73029E-5*
let-7b-5p	0.53	*1.74428E-4*
miR-16-5p	0.43	*0.00291*
miR-26b-5p	0.43	*0.0034*

Fig S7. Positive correlation between the levels of circulating and tissue-expressed miRNAs in the mouse model of rCDI. Correlation of miRNAs suppressed by rCDI and upregulated by FMT as assessed by Spearman's rank coefficient (and statistical significance). Upper panel, example of linear fitting for miR-150-5p levels in matched sera and ceca of individual animals.

Supplementary Figure 8.

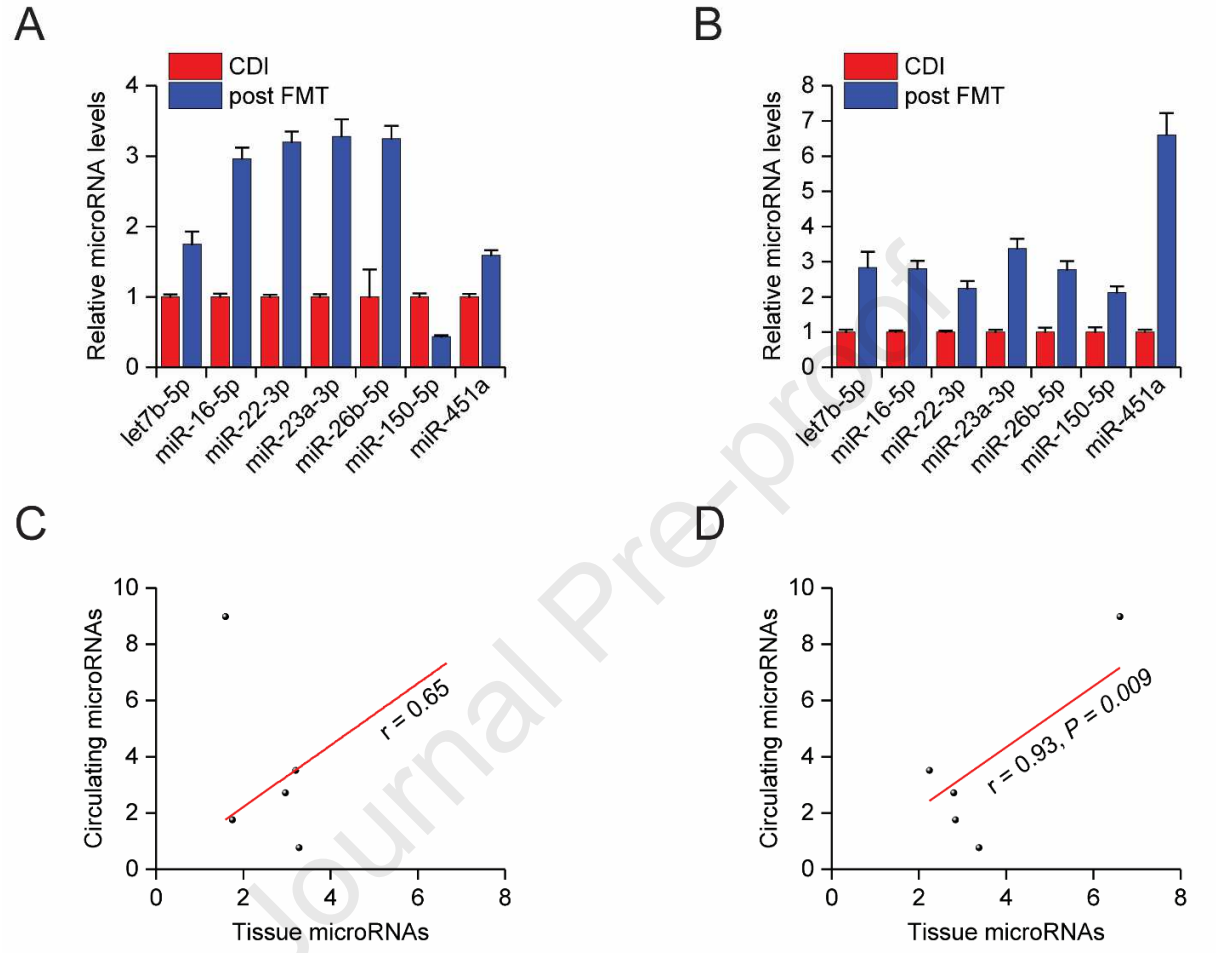

Fig S8. Positive correlation between the levels of circulating and tissue-expressed miRNAs in an 84-year old male patient with fulminant CDI pre and post FMT delivered by colonoscopy. *(A-B)* Changes in tissue miRNA levels in biopsies from *(A)* ascending and *(B)* descending colon pre and post FMT. *(C-D)* Correlation of changes in the levels of circulating miRNAs upregulated by FMT with changes in *(C)* ascending and *(D)* descending colonic tissue-expressed miRNAs in the same patient. MicroRNA levels were assessed by RT-qPCR and normalized against RNU1A1 and 5S rRNA for tissues and RNU1A1 and cel-miR-39 (spike-in) for sera and are expressed as mean ± s.e.m. compared to control samples, set as 1. Correlations were assessed by Spearman's rank coefficient.

Supplementary Figure 9.

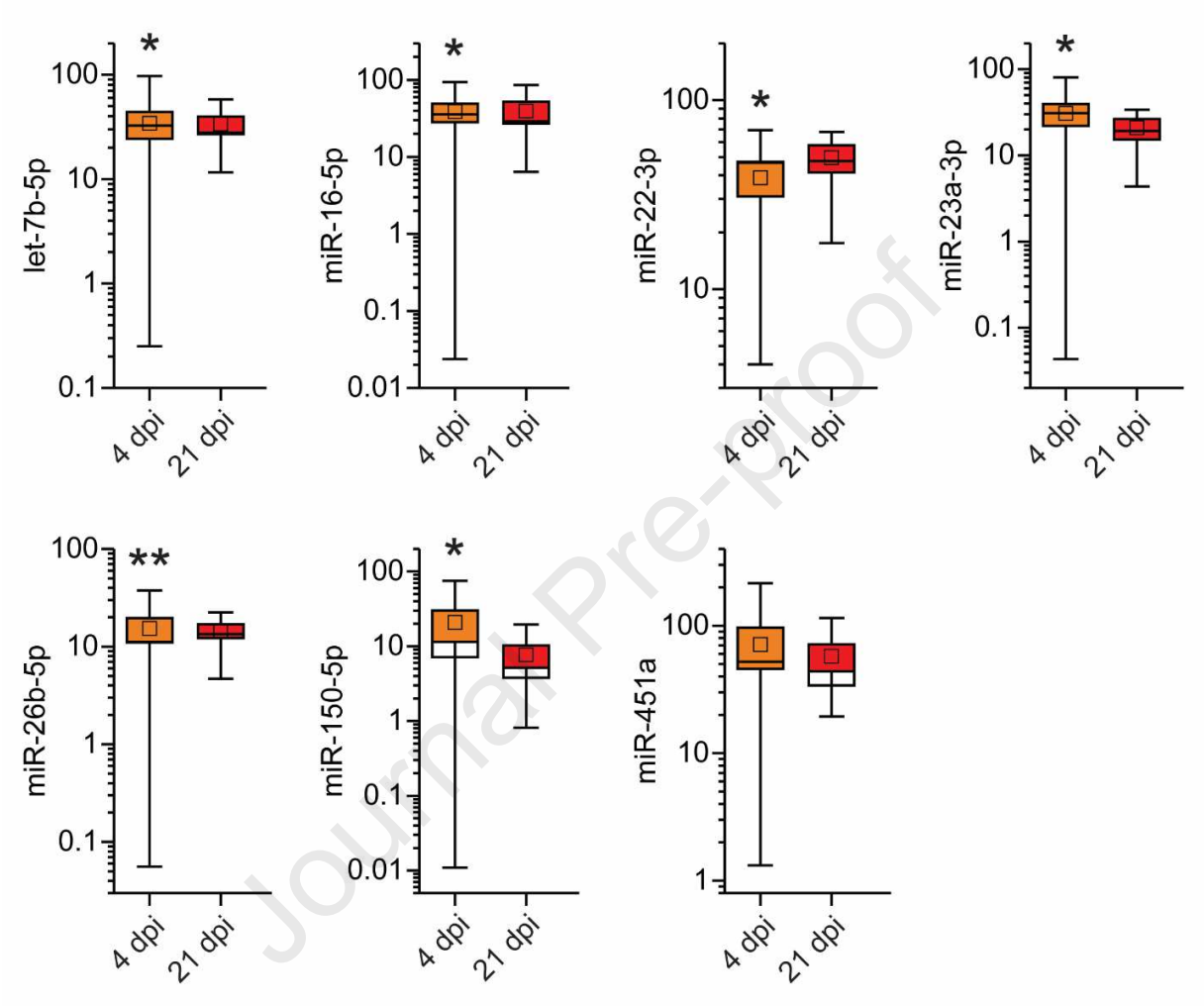

Fig S9. Effects of *C. difficile* strain 630 on intestinal tissue miRNAs in a mouse model of recurrent CDI. Box plots depicting the changes in miRNA levels in ceca from mice infected with *C. difficile*, 4- and 21-days post infection (dpi). Box plots denote mean % change ± s.e.m., inner boxes represent mean, and error bars represent 95% confidence interval. miRNA levels were assessed by RT-qPCR normalized against RNU5G and 5S rRNA, and compared to control group (FMT donors), set as 100%. Statistical significance was determined by Student's *t*-test, *$P < 0.05$, **$P < 0.01$ (compared to donor). The 21 dpi data (statistical analysis provided in Fig. 2B) are included for comparisons.

Supplementary Figure 10.

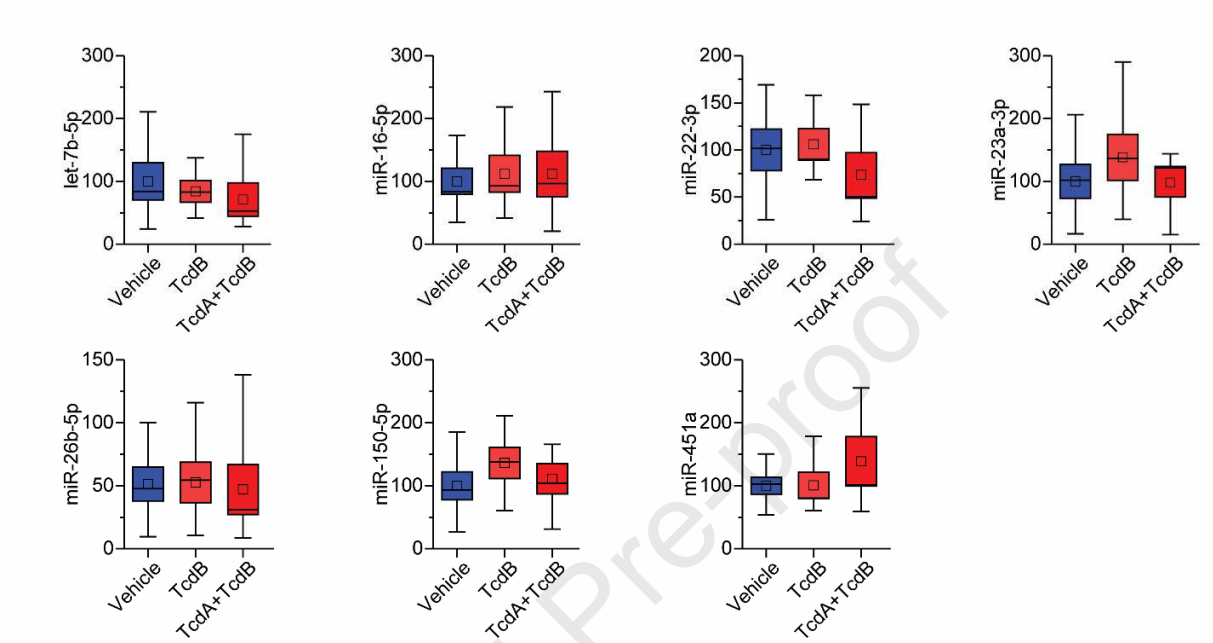

Fig S10. Circulating miRNAs in mice treated by intrarectal instillation with *C. difficile* whole toxins (derived from VPI 10463 reference strain). Box plots depicting the changes in miRNA levels in sera from animals treated with TcdB, combination of TcdA with TcdB, compared to HBSS-treated controls (Vehicle). Box plots denote mean % change ± s.e.m., inner boxes represent mean, and error bars represent 95% confidence interval. miRNA levels were assessed by RT-qPCR and were normalized against RNU1A1 and cel-miR-39, and compared to control samples, set as 100%.

Supplementary Figure 11.

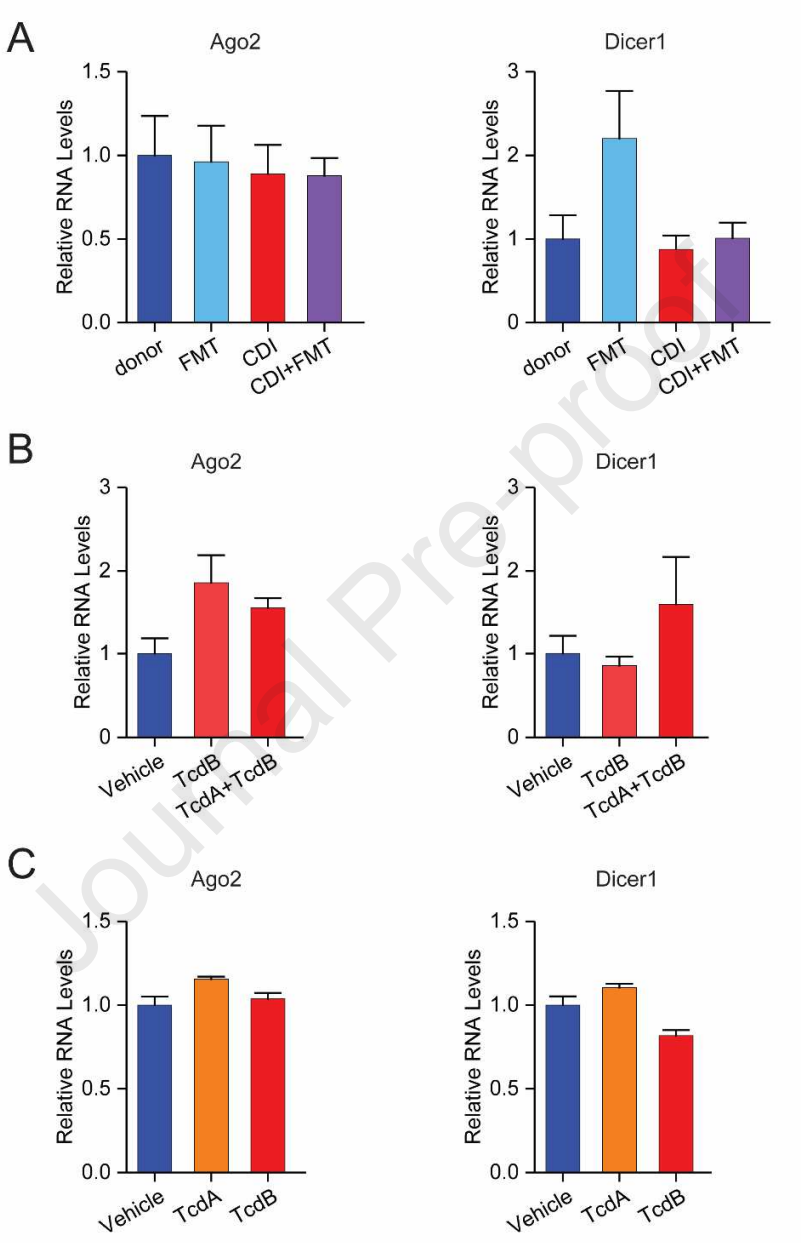

Fig S11. Effects of *C. difficile* infection on Ago2 and Dicer1 expression. Ago2 and Dicer1 mRNA levels in *(A)* ceca from animals treated with FMT, infected with *C. difficile* (CDI), and infected with *C. difficile* and treated with FMT (CDI+FMT), compared to FMT donors, *(B)* colonic tissues from animals treated with TcdB or combination of TcdA with TcdB, compared to controls (Vehicle), *(C)* colonoids treated with TcdA or TcdB, compared to DMEM-treated

controls (Vehicle). mRNA levels assessed by RT-qPCR were normalized against beta-Actin and GAPDH and are expressed as mean± s.e.m. compared to control samples, set as 1.

Supplementary Figure 12.

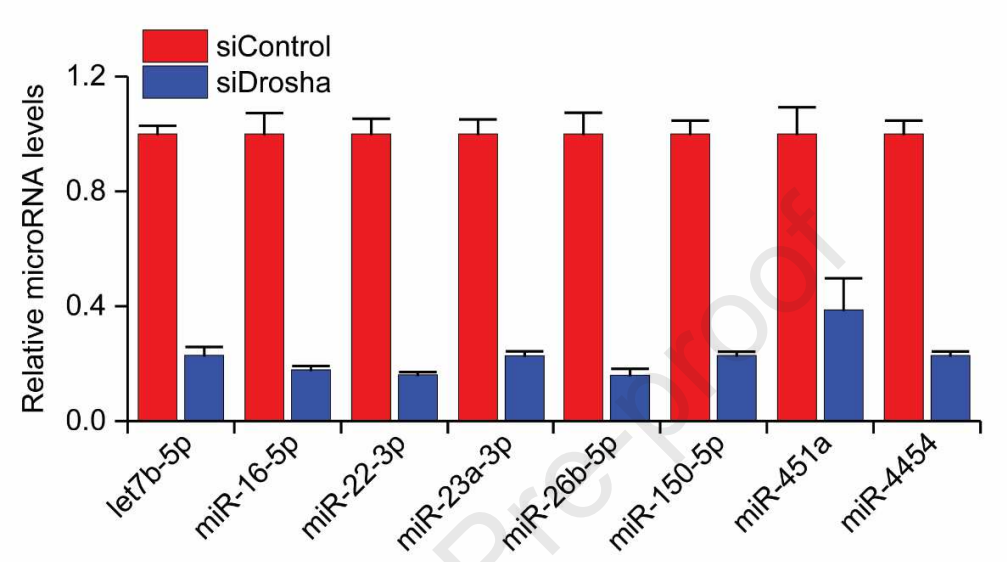

Fig S12. miRNA levels in NCM356 cells upon knockdown of Drosha. Drosha was knocked down by means of siRNA (5nM) and 48h later miRNA levels were assessed by RT-qPCR. Data expressed as mean ± s.e.m. compared to control non-targeting siRNA (siControl) transfected cells, set as 1.

Supplementary Figure 13.

	Circulating Proteins			
Circulating microRNAs	**IL12B**	**IL18**	**FGF21**	**TNFRSF9**
miR-23a-3p	**-0.220 (0.032)**		-0.284 (0.005)	
miR-150-5p		**-0.226 (0.028)**		
miR-26b-5p			**-0.305 (0.003)**	
miR-130a-3p			-0.257 (0.012)	
miR-20a-5p+miR 20b-5p				-0.205 (0.046)
miR-28-5p				**-0.238 (0.020)**

Fig S13. Inverse correlation between the circulating levels of miRNAs and protein levels of their predicted targets. Correlation of miRNAs upregulated by FMT with predicted target cytokines/chemokines as assessed by Spearman's rank coefficient (and statistical significance). Highlighted in red the interactions validated experimentally by RT-qPCR and 3'UTR activity reporter assays, after miRNA overexpression in colonic epithelial cells (Figure 5).

Supplementary Figure 14.

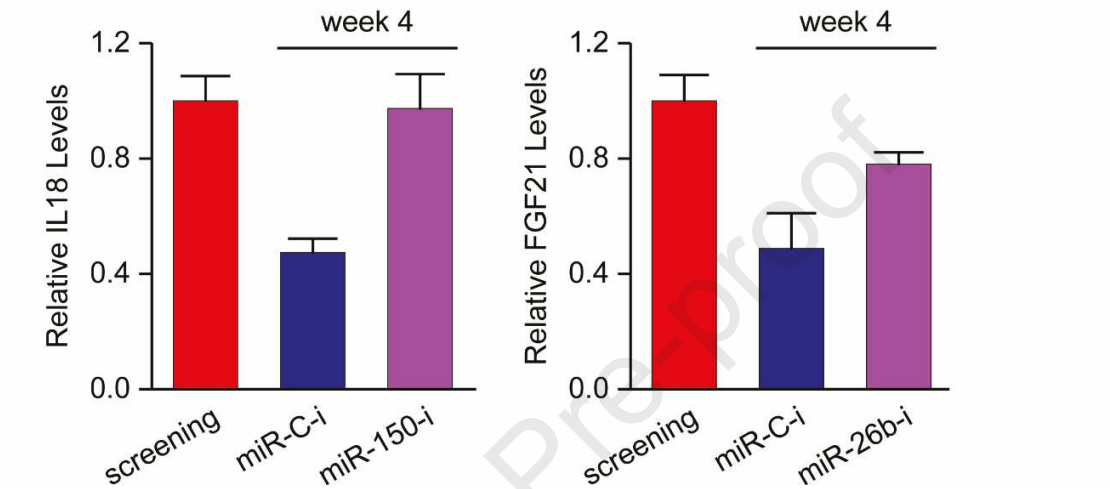

Fig S14. Functional effects of Fecal Microbiota Transplantation (FMT)-regulated circulating miRNAs in patients with *C. difficile* infection. PBMCs derived from a patient 4 weeks post FMT were treated with miRNA inhibitors and analyzed for the levels of their respective targets 24 hours later. The RNA levels of IL18 and FGF21 were assessed by RT-qPCR, normalized against beta-Actin and GAPDH levels and are expressed as mean ± s.e.m. compared to PBMCs collected at screening (pre-FMT), set as 1. miR-C-i, a non-targeting miRNA inhibitor, was used as control.

Supplementary Figure 15.

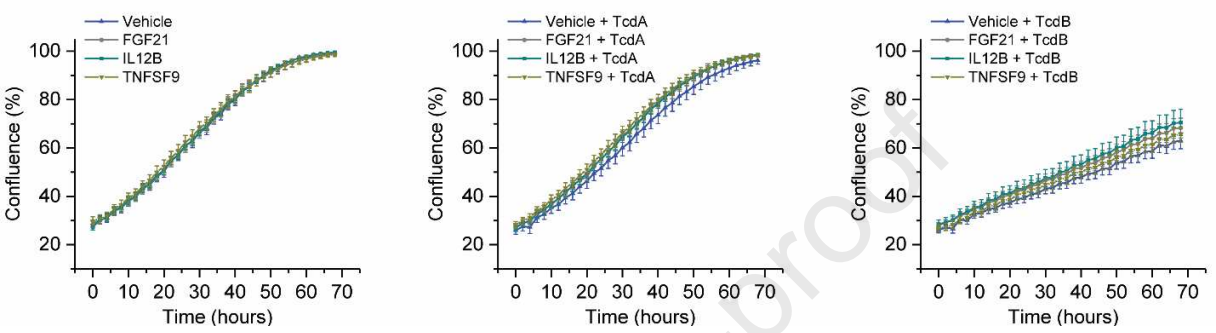

Fig S15. Effects of cytokines regulated by FMT in combination with *C. difficile* exotoxins (VPI 10463 reference strain) on epithelial cell growth. NCM356 cells pretreated with FGF21, IL12B and TNFSF9 (50ng/ml) or Vehicle where exposed to 10pM TcdA (middle panel) or TcdB (right panel) and cell growth was monitored in real time and expressed as % of confluence (IncuCyte).

Supplementary Figure 16.

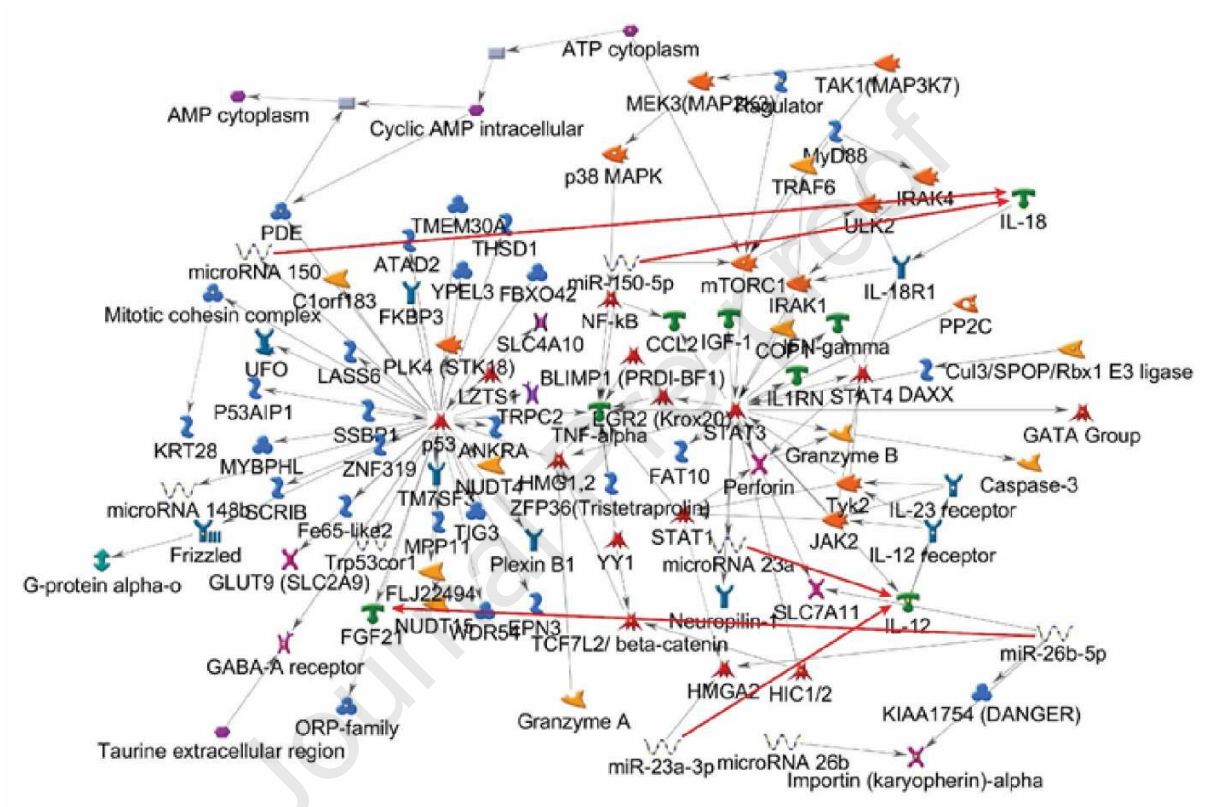

Fig S16. The effects of miR-23a, miR-150 and miR-26b on IL12B, IL18 and FGF21, respectively, provide novel links between metabolic and inflammatory networks. The miRNA-regulated pathways with the new links (red arrows), assessed using the Metacore network analysis software.

Supplementary Figure 17.

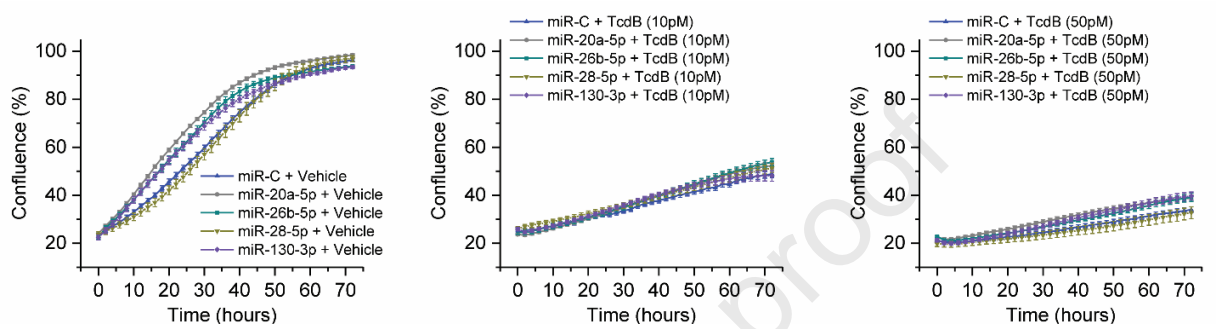

Fig S17. Effects of microRNAs regulated by FMT in combination with TcdB on epithelial cell growth. NCM356 cells transfected with miR-20a-5p, miR-26b-5p, miR-28-5p, miR-130a-3p or miR-C, where exposed to 10pM (middle panel) or 50pM (right panel) of TcdB or Vehicle (left panel) and cell growth was monitored in real time and expressed as % of confluence (IncuCyte). miR-C (cel-miR-39-3p), a non-targeting miRNA, was used as negative control.

Supplementary Figure 18.

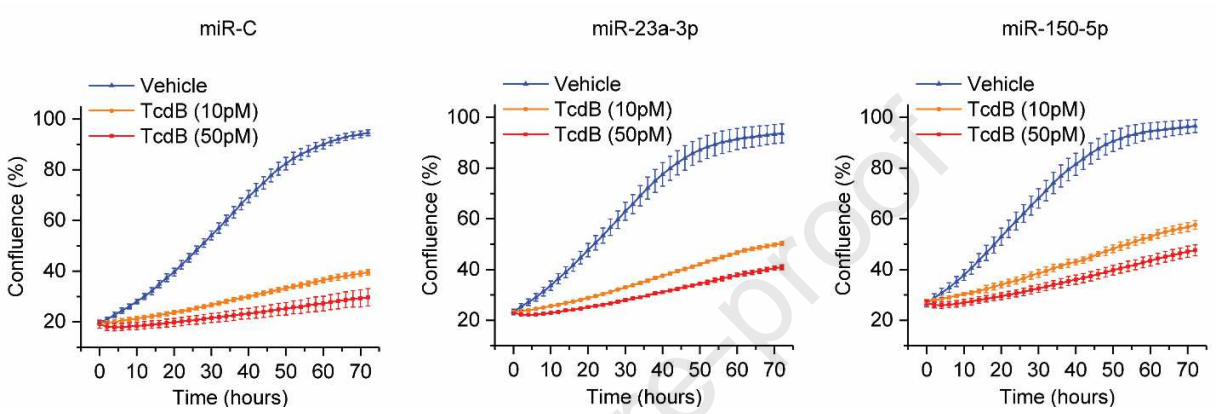

Fig S18. Effects of microRNAs regulated by FMT in combination with TcdB on epithelial cell growth. NCM356 cells transfected with miR-23a-3p, miR-150-5p or miR-C, where exposed to TcdB or Vehicle (left panel) and cell growth was monitored in real time and expressed as % of confluence (IncuCyte). miR-C (cel-miR-39-3p), a non-targeting miRNA, was used as negative control.

Supplementary Figure 19.

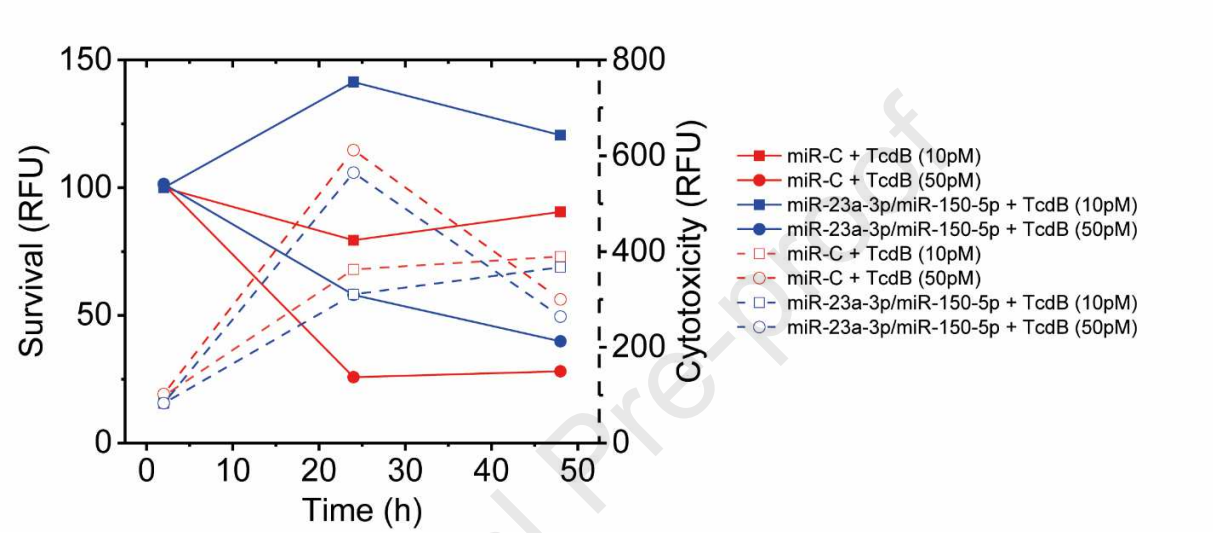

Fig S19. Effects of microRNAs regulated by FMT on TcdB-induced cytotoxicity and cell survival. NCM356 cells transfected with miR-23a-3p and miR-150-5p or miR-C, where exposed to TcdB and cytotoxicity and survival was monitored using the Apotox Glo assay. Results are expressed as % survival (solid lines) or ratio of cytotoxicity against surviving cells (dotted lines). miR-C (cel-miR-39-3p), a non-targeting miRNA, was used as negative control.

Supplementary Figure 20.

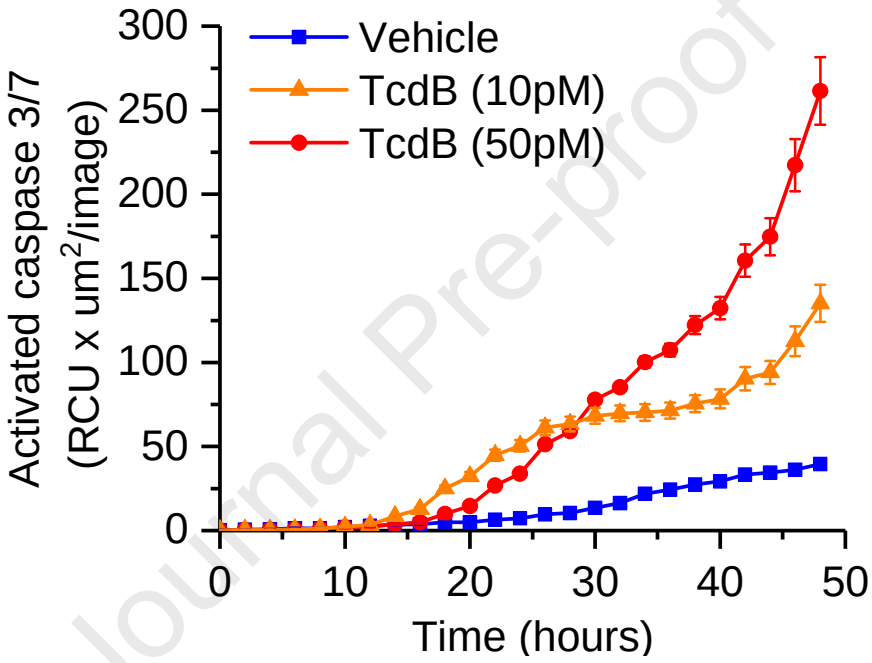

Fig S20. Effects of TcdB on cell apoptosis. NCM356 where exposed to TcdB and apoptosis was monitored in real-time as activated caspase3/7 fluorescence (IncuCyte).

Supplementary Figure 21.

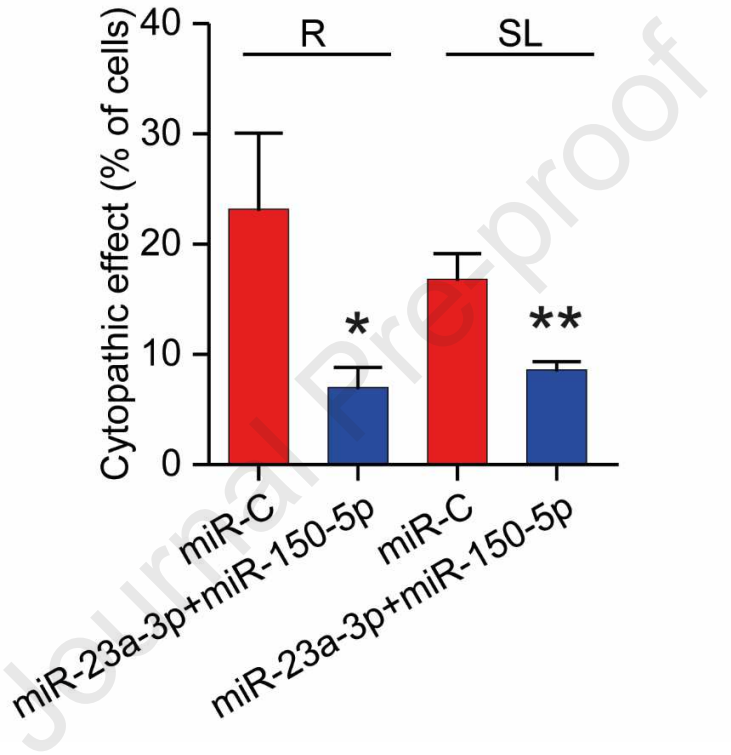

Fig S21. Effects of miR-23a-3p and miR-150-5p overexpression on TcdB-mediated cytoskeleton rearrangements. NCM356 cytoskeleton organization was studied by fluorescence microscopy after phalloidin staining. Cells were scored by two independent researchers blind to the treatments and the ratio of morphologically altered cells were expressed as % of the total number of cells per field. miR-C (cel-miR-39-3p), a non-targeting miRNA, was used as negative control. Statistical significance was determined by Student's t-test, *P < 0.05, **P < 0.01. R, rounded cells; SL, spindle like cells.

	Discovery Cohort - NCT02254811			Replication Cohort - NCT01398969		
	Capsule (n = 25)	Colonoscopy (n = 17)	*P* value	Fresh (n = 11)	Frozen (n = 13)	*P* value
Age, mean (SD), y	59.0 (19.7)	56.4 (18.7)	0.6624	74.3 (14.1)	71.6 (18.6)	0.7363
Females, No. (%)	21 (84.0%)	9 (52.9%)	0.0659	4 (36.4%)	9 (69.2%)	0.2305
Charlson comorbodity index, median	3 (2-5)	3 (0-4)	0.4353			
Immunosuppressed patients, No. (%)	2 (8.0%)	3 (17.6%)	0.6439	3 (27.3%)	1 (7.7%)	0.4637
Use of immune modulator, No. (%)						
Costicosteroid	0 (0%)	1 (5.9%)	0.8443			
Immunosuppresant	1 (4.0%)	1 (5.9%)	1	4 (36.4%)	3 (23.1%)	0.7926
Biologic	2 (8.0%)	1 (5.9%)	1	5 (45.5%)	4 (30.8%)	0.751
Body mass index (BMI), mean (SD)	25.3 (6.6)	27.0 (4.1)	0.3113			
Inpatient status at screening, No. (%)	3 (12%)	0 (0%)	0.3833	7 (63.6%)	6 (46.2%)	0.6561
PPI use prior to FMT, No. (%)	4 (16%)	1 (5.9%)	6111	5 45.5%)	5 (38.5%)	1
No. of RCDI episodes prior to FMT; median	3 (3-4)	3 (3-4)	0.3893	3 (2.5-4.0)	3 (3-4)	0.4641
Duration of RCDI prior to FMT, median	65 (49-96)	70 (57-135)	0.2648			
No. of CDI related hospital admissions, med	1 (0-2)	0 (0--0)	0.0057			
IBD, No. (%)						
Ulcerative colitis	2 (8.3%)	3 (1.8%)	0.6439			
Crohn's	2 (8.3%)	1 (5.9%)	1	2 (18.2%)	2 (15.4%)	1
Hemoglobin (g/dL), median	137 (129-144)	138 (132-144)	0.6079			
WBC (10^9/L), median	8 (6.8-8.6)	6.5 (5.1-6.9)	0.0143	15.30 (8.35-21.70)	8.9 (6.7-12.6)	0.2212
Albumin (g/L), median	40.5 (38.8-43.3)	40 (38-42)	0.5857	31 (28-34)	30 (24-34)	0.8557
CRP (mg/L), median	1.9 (0.9-5.8)	6.2 (1.3-10.2)	0.244			
Creatinine (mg/dL), median	70 (58.75-76)	70 (59-84)	0.7404	88 (69.5-127)	85 (64-128)	0.6849

Table 1. Participant baseline characteristics for the discovery and replication cohorts